

FINAL REPORT

INVESTIGATION OF THE EFFECTS OF ACID DEPOSITION ON MATERIALS

Contract Nos. A4-110-32 and A5-137-32

Prepared for

California Air Resources Board
P.O. Box 2815
Sacramento, CA 95812

by

Combustion Engineering Environmental's
Environmental Monitoring & Services, Inc.
4765 Calle Quetzal
Camarillo, CA 93010

R. Vijayakumar*

and

University of Southern California
Los Angeles, CA 90089

F. Mansfeld
R. Henry

JUNE 1989

*presently with Cambridge Filter Corporation

ABSTRACT

Damage functions have been obtained for materials of economic significance which had been exposed between March 1986 and March 1988 at three sites in Southern California (Burbank, Long Beach and Upland), and a background site in Central California (Salinas). These damage functions relate the atmospheric corrosion loss to the concentration of routinely measured pollutants. The materials exposed were galvanized steel, nickel, two types of flat latex exterior house paint, aluminum, nylon fabric, polyethylene and concrete. Due to experimental problems with the concrete bricks and difficulties in determining corrosion damage for the polyethylene, damage functions are not available for these materials.

The exposure tests have been supported by laboratory experiments in which corrosion damage has been determined under carefully controlled conditions for single pollutants such as SO_2 , NO_2 and O_3 , and their combinations, and for HNO_3 aerosol. Significant damage was observed only in the presence of SO_2 or the HNO_3 aerosol.

At both the field and the laboratory tests atmospheric corrosion rate monitors (ACRM) have been exposed to provide a continuous record of the corrosion behavior. The ACRM data confirmed the results from the field tests that corrosion rates at the sites in Southern California were higher in the summer months than in the winter months. Statistical analysis of these data has shown that this behavior, which is different from that observed in most other exposure studies performed in Europe and elsewhere, is probably due to the very low SO_2 concentrations and the formation of gaseous HNO_3 as well as nitrate and sulfate particulates in the summer by photochemical reactions.

ACKNOWLEDGEMENTS

A program of the complexity and difficulty of this study could not be completed without the help of a large number of dedicated people. Among them were:

Samuel Jeanjaquet, who carried out the laboratory experiments at the Rockwell International Science Center (RISC) and handled the Atmospheric Corrosion Rate Monitor (ACRM) data tapes from the field sites from the first year of this project,

Guangmei Chen, who carried out the laboratory experiments at the Corrosion and Environmental Effects Laboratory/University of Southern California (CEEL/USC),

John White, who provided software for the analysis of the ACRM data at USC and RISC and helped with the analysis of data at CEEL/USC,

Wongwook Won, who handled all the ACRM data tapes at CEEL/USC,

Dr. Hong Shih, Research Associate at CEEL/USC, who provided guidance to the CEEL students involved in this project and made major contributions to the analysis of the ACRM and RH data,

Dwight Landis of Atmospheric Technology, ATEC for donation of the laboratory test chamber used at USC,

Robert Cary of Sunset Laboratories, who built and donated service on the Atmospheric Corrosion Rate Monitor data Logger (ACRMDL),

Christine Ladisch, Associate Professor of Textile Science at Purdue University, who provided expert advice concerning nylon fabric specimen preparation procedures and conducted the breaking strength measurements,

R. Samuel Williams, Research Chemist in Wood Surface Chemistry and Property Enhancement for the USDA Forest Service, who provided essential information on selection and preparation of wood for use in painted specimens,

Dr. Leo Topol of Combustion Engineering Environmental's Environmental Monitoring and Services, Inc. (EMSI) who was the initial principal investigator and helped edit the report,

Richard Harris, who performed field, laboratory, data processing, and report editing tasks at EMSI,

Wilma Seltzer, who helped edit the report at EMSI,

Susan Luke, Timothy Nelsen, Chris Massingal and Randal Horne, who performed field and laboratory tasks at EMSI,

ACKNOWLEDGEMENTS (continued)

Robert Hillestad, who managed field and laboratory operations at EMSI, assisted in writing the report and was program manager at the conclusion of the project,

Marian Dempsey, Elaine Houston and Patti Miller at EMSI, who typed and retyped the report,

Finally, we wish to acknowledge the support and guidance of Manjit Ahuja of the California Air Resources Board as our project officer.

This report was submitted in fulfillment of A4-110-32 and A5-137-32 "Investigation of Effects of Acid Deposition on Materials" by Environmental Monitoring & Services, Inc., under the sponsorship of the California Air Resources Board. Work was completed as of June 1989.

DISCLAIMER

"The statements and conclusions in this report are those of the contractor and not necessarily those of the California Air Resources Board. The mention of commercial products, their source or their use in connection with material reported herein is not to be construed as either an actual or implied endorsement of such products".

TABLE OF CONTENTS

	<u>Page</u>
Abstract	
Acknowledgements	
Disclaimer	
Table of Contents	
List of Figures	
List of Tables	
Summary and Conclusions	
Recommendations for Future Research	
1.0 Introduction.....	1
2.0 Project Design.....	3
2.1 Materials Selection.....	4
2.2 Measurement of Damage.....	10
2.3 Field Exposure.....	15
2.4 Laboratory Experiments.....	24
3.0 Results and Discussion.....	28
3.1 Field Measurements.....	28
3.1.1 Weight Loss Data.....	28
3.1.1.1 Galvanized Steel.....	28
3.1.1.2 Nickel.....	30
3.1.1.3 House Paint.....	30
3.1.1.4 Aluminum.....	35
3.1.2 Strength Loss of Fabric.....	35
3.1.3 Conclusions.....	35
3.1.4 Atmospheric Corrosion Rate Monitors (ACRM).....	39
3.1.5 Appearance Measurements.....	45
3.1.5.1 Paint on Stainless Steel.....	55
3.1.5.2 Paint on Wood.....	55
3.1.6 Aerometric Measurements.....	56
3.2 Laboratory Tests.....	70
3.2.1 Coupon Exposure.....	70
3.2.2 ACRM Exposure.....	74
3.2.3 Statistical Analysis.....	78
3.2.3.1 Weight Loss Data.....	78
3.2.3.2 ACRM Data.....	84

TABLE OF CONTENTS (continued)

	<u>Page</u>
4.0 Damage Functions.....	88
4.1 Analysis of Weight Loss Data.....	88
4.2 Analysis of ACRM Data.....	94
4.2.1 Comparison of Weight Loss Rates and ACRM Data.....	94
4.2.2 Seasonal Variations of the ACRM Data.....	96
4.2.3 Relationships of ACRM Data with Air Quality and Meteorological Variables.....	98
4.2.4 Summary of ACRM Analysis Results.....	103
4.3 Damage Functions for Galvanized Steel, Aluminum and High Carbonate Paint.....	103
4.4 Damage Functions for Other Materials.....	105
5.0 References.....	108
List of Inventions Report and Publications.....	110
Glossary of Terms, Abbreviations and Symbols.....	111
Appendix.....	112

LIST OF FIGURES

<u>Figure</u>		<u>Page</u>
2-1	SITE LOCATION MAP.....	18
2-2	FIELD SAMPLE EXPOSURE SCHEDULE.....	22
2-3a	FIELD SITE PHOTOGRAPH OF SPECIMEN RACK, UPLAND.....	23
2-3b	CLOSE UP OF SPECIMEN RACK.....	23
2-4	LABORATORY ACID DEPOSITION CHAMBER.....	26
3-1	WEIGHT LOSS VS. TIME FOR GALVANIZED STEEL, FIRST SET.....	29
3-2	WEIGHT LOSS VS. TIME FOR GALVANIZED STEEL, BURBANK SITE.....	31
3-3	WEIGHT LOSS VS. TIME FOR NICKEL, FIRST SET.....	32
3-4	WEIGHT LOSS VS. TIME FOR NICKEL, BURBANK SITE.....	33
3-5	WEIGHT LOSS VS. TIME FOR PAINT WITH CARBONATE EXTENDER, FIRST SET.....	34
3-6	WEIGHT LOSS VS. TIME FOR PAINT WITHOUT CARBONATE EXTENDER, FIRST SET.....	36
3-7	WEIGHT LOSS VS. TIME FOR ALUMINUM, FIRST SET.....	37
3-8	REDUCTION IN BREAKING STRENGTH FOR NYLON FABRIC.....	38
3-9a	BURBANK MONTHLY AVERAGES FOR T70 and T80	42
3-9b	BURBANK MONTHLY AVERAGES FOR T_{corr} FROM ZINC ACRM SENSORS.....	43
3-9c	BURBANK MONTHLY AVERAGES FOR T_{corr} FROM NICKEL ACRM SENSORS.....	43
3-9d	BURBANK MONTHLY CORROSION LOSS FROM ZINC ACRM SENSOR.....	44
3-9e	BURBANK MONTHLY CORROSION LOSS FROM NICKEL ACRM SENSOR.....	44
3-10a	LONG BEACH MONTHLY AVERAGES FOR T70 AND T80.....	46

LIST OF FIGURES (continued)

<u>Figure</u>		<u>Page</u>
3-10b	LONG BEACH MONTHLY AVERAGES FOR T_{corr} FROM ZINC ACRMS SENSORS.....	47
3-10c	LONG BEACH MONTHLY AVERAGES FOR T_{corr} FROM NICKEL ACRM SENSORS.....	47
3-10d	LONG BEACH MONTHLY CORROSION LOSS FROM ZINC ACRM SENSORS.....	48
3-10e	LONG BEACH MONTHLY CORROSION LOSS FROM NICKEL ACRM SENSORS.....	48
3-11a	UPLAND MONTHLY AVERAGES FOR T70 AND T80.....	49
3-11b	UPLAND MONTHLY AVERAGES FOR T_{corr} FROM ZINC ACRM SENSORS.....	50
3-11c	UPLAND MONTHLY AVERAGES FOR T_{corr} FROM NICKEL ACRM SENSORS.....	50
3-11d	UPLAND MONTHLY CORROSION LOSS FROM ZINC ACRM SENSOR.	51
3-11e	UPLAND MONTHLY CORROSION LOSS FROM NICKEL ACRM SENSOR.....	51
3-12a	SALINAS MONTHLY AVERAGES FOR T70 AND T80.....	52
3-12b	SALINAS MONTHLY AVERAGES FOR T_{corr} FROM ZINC ACRM SENSORS.....	53
3-12c	SALINAS MONTHLY AVERAGES FOR T_{corr} FROM NICKEL ACRM SENSORS.....	53
3-12d	SALINAS MONTHLY CORROSION LOSS FROM ZINC ACRM SENSORS.....	54
3-12e	SALINAS MONTHLY CORROSION LOSS FROM NICKEL ACRM SENSORS.....	54
3-13a	BURBANK AVERAGE MONTHLY CONCENTRATION VALUES OF O_3 AND NO_2 FOR TWO YEAR EXPOSURE PERIOD.....	57
3-13b	LONG BEACH AVERAGE MONTHLY CONCENTRATION VALUES OF O_3 AND NO_2 FOR TWO YEAR EXPOSURE PERIOD.....	57

LIST OF FIGURES (continued)

<u>Figure</u>		<u>Page</u>
3-13c	SALINAS AVERAGE MONTHLY CONCENTRATION VALUES OF O ₃ AND NO ₂ FOR TWO YEAR EXPOSURE PERIOD.....	58
3-13d	UPLAND AVERAGE MONTHLY CONCENTRATION VALUES OF O ₃ AND NO ₂ FOR TWO YEAR EXPOSURE PERIOD.....	58
3-14a	BURBANK AVERAGE MONTHLY HNO ₃ CONCENTRATIONS FOR TWO YEAR EXPOSURE PERIOD.....	59
3-14b	UPLAND AVERAGE MONTHLY HNO ₃ CONCENTRATIONS FOR TWO YEAR EXPOSURE PERIOD.....	60
3-14c	LONG BEACH AVERAGE MONTHLY HNO ₃ CONCENTRATIONS FOR TWO YEAR EXPOSURE PERIOD.....	61
3-14d	SALINAS AVERAGE MONTHLY HNO ₃ CONCENTRATIONS FOR TWO YEAR EXPOSURE PERIOD.....	62
3-15	MONTHLY AVERAGE SULFUR DIOXIDE LEVELS.....	64
3-16	MONTHLY AVERAGE NO _x LEVELS.....	65
3-17	MONTHLY AVERAGE OZONE LEVELS.....	67
3-18	MONTHLY AVERAGE T60.....	68
3-19	MONTHLY AVERAGE PERCENT RELATIVE HUMIDITY.....	69
3-20	TEST CHAMBER OUTLET CONCENTRATIONS OF SO ₂ AND NO ₂ ...	75
3-21	ZINC SENSOR VS. WEIGHT LOSS FOR GALVANIZED STEEL COUPONS.....	86
3-22	ACRM DETERMINATION OF ZINC SENSOR VS. WEIGHT LOSS FOR GALVANIZED STEEL COUPONS.....	87
4-1	APPROXIMATE STARTING AND ENDING TIME FOR THE TWELVE EXPOSURE GROUPS.....	89
4-2	AVERAGE GALVANIZED STEEL WEIGHT LOSS RATES AT BURBANK, LONG BEACH, UPLAND AND SALINAS SITES.....	90
4-3	AVERAGE NICKEL WEIGHT LOSS RATES AT BURBANK, LONG BEACH, UPLAND, AND SALINAS SITES.....	91

LIST OF FIGURES (continued)

<u>Figure</u>		<u>Page</u>
4-4	AVERAGE PAINT WITH CARBONATE EXTENDER WEIGHT LOSS RATES AT BURBANK, LONG BEACH, UPLAND, SALINAS SITES.	92
4-5	AVERAGE PAINT WITHOUT CARBONATE EXTENDER WEIGHT LOSS RATES AT BURBANK, LONG BEACH, UPLAND, SALINAS SITES.	93
4-6	NICKEL WEIGHT LOSS RATE VS NICKEL UP SENSOR DATA....	95
4-7	CUMULATIVE CORROSION LOSS FOR NICKEL UP SENSOR AT LONG BEACH.....	97

LIST OF TABLES

<u>Table</u>	<u>Page</u>
2-1 RANKING OF MATERIALS BY ECONOMIC LOSSES DUE TO AIR POLLUTION DAMAGE AND SOILING.....	6
2-2 ANNUAL SITE POLLUTION LEVEL (1982-1984 Average).....	17
2-3 AVERAGE ANNUAL CLIMATIC DATA FROM STATIONS REPRESENTING THE FIELD SITES.....	20
3-1 AVAILABLE DAYS/MONTHS OF ACRM DATA.....	41
3-2 CONDITIONS FOR TEST SERIES AT ROCKWELL INTERNATIONAL SCIENCE CENTER (SC) AND UNIVERSITY OF SOUTHERN CALIFORNIA (USC).....	71
3-3 WEIGHT LOSS DATA FOR LABORATORY TESTS AND LOSS OF STRENGTH FOR NYLON TEXTILE.....	72
3-4 SUMMARY OF ACRM DATA -- LABORATORY TESTS (SC AND USC TEST SERIES).....	76
3-5 ONE-WAY ANALYSIS OF VARIANCE OF WEIGHT LOSS FOR GALVANIZED STEEL.....	80
3-6 ONE-WAY ANALYSIS OF VARIANCE OF WEIGHT LOSS FOR NICKEL.....	80
3-7 ONE-WAY ANALYSIS OF VARIANCE OF WEIGHT LOSS FOR PAINT WITHOUT CARBONATE EXTENDER.....	81
3-8 ONE-WAY ANALYSIS OF VARIANCE OF WEIGHT LOSS FOR PAINT WITH CARBONATE EXTENDER.....	81
3-9 ONE-WAY ANALYSIS OF VARIANCE OF WEIGHT LOSS FOR ALUMINUM.....	82
3-10 ONE-WAY ANALYSIS OF VARIANCE OF STRENGTH LOSS FOR NYLON TEXTILE.....	82
3-11 SUMMARY OF THE LABORATORY EXPOSURE RESULTS.....	83
4-1 VARIABLES USED IN ANALYSIS OF ACRM DATA.....	99
4-2 PRINCIPAL COMPONENT ANALYSIS OF BURBANK AIR QUALITY AND METEOROLOGICAL DATA.....	100

LIST OF TABLES (continued)

<u>Table</u>		<u>Page</u>
4-3	COEFFICIENTS FOR DAMAGE FUNCTIONS FOR CURRENT POLLUTION LEVELS AT SOUTHERN CALIFORNIA SITES.....	106
4-4	COEFFICIENTS FOR DAMAGE FUNCTIONS FOR CURRENT POLLUTION LEVELS AT ALL CALIFORNIA SITES.....	107

APPENDIX

<u>Figure</u>		<u>Page</u>
A-1	SPECIMEN PUNCHED HOLE IDENTIFICATION NUMBERING SYSTEM.....	116
A-2	IDENTIFICATION TEMPLATE.....	123
A-3	RECTANGULAR SHAPED TEST CHAMBER.....	124
A-4a	FIELD SITE PHOTOGRAPH OF SPECIMEN RACK, UPLAND.....	133
A-4b	CLOSE UP OF SPECIMEN RACK.....	133
A-5	FIELD EXPOSURE RACK DIAGRAM.....	134
A-6	LABORATORY ACID DEPOSITION CHAMBER.....	137
A-7	ACRM SENSOR INSTALLED ON EXPOSURE RACK AND FACING DOWN.....	139

SUMMARY AND CONCLUSIONS

Exposure tests have been carried out between March 1986 and March 1988 at three test sites in Southern California (Burbank, Long Beach and Upland) and at a background site in Central California (Salinas). The objective of this project was to determine damage functions which relate the atmospheric corrosion losses to the concentration of the pollutants which are routinely monitored. These damage functions in conjunction with the results of an inventory of the material studied can then be used to estimate the economic losses due to acid deposition. The materials investigated in this study were chosen based on their economic importance and included galvanized steel, nickel, aluminum, two types of flat latex exterior housepaint, nylon fabric, polyethylene and concrete. Atmospheric data were provided by ARB's air monitoring network at the test sites.

The field sites have been supported by laboratory tests in which corrosion damage was determined under carefully controlled conditions. A 6-hour diurnal cycle was used in which the samples were chilled for 1.5h to induce condensation. The samples were exposed to SO_2 , NO_2 or O_3 and their combinations and to HO_3 aerosol of two different concentrations and flow rates.

In both the field tests and the laboratory tests atmospheric corrosion rate monitors (ACRM) were exposed. These gave a continuous record of the corrosion behavior of the sensor materials which were zinc and nickel. At the field sites the ACRMs were exposed in two positions, facing the sky and facing the ground. A relative humidity (RH) and temperature probe was also exposed at each site. ACRM, RH and temperature data were collected every 10 min. and stored on magnetic tape. Software developed for this project was used for the display and analysis of these data.

The results from the field tests in Southern California are quite different from those which have been reported in Europe and other parts

considered, but either performed poorly or were not physically reasonable. It should be noted that O_3 and NO_2 themselves did not cause damage - as shown in the laboratory tests, but are surrogates for the components of photochemical smog that presumably caused damage such as HNO_3 vapor, organic acids and acidic particles. Two sets of damage functions were determined. The first was derived from weight loss data from the Southern California sites. These damage functions have non-linear terms, such as $O_3 \times T^{60}$, and as a result may predict unreasonable corrosion rates if applied to other geographic areas or to time periods other than annual or seasonal averages. Development of a more general set of damage functions was hampered by the frequent loss of relative humidity data at the background site in Salinas. However, by consolidating all the Salinas data into a single set of averages, a second set of damage functions was estimated. This second set may be valid for a wider range of conditions than the first set, and since it does not use non-linear functions, application to other areas and conditions will not produce physically impossible corrosion rate predictions. However, the second set of damage functions does not fit the observed weight loss data for Southern California as well as the first.

RECOMMENDATIONS FOR FUTURE RESEARCH

By discovering important differences between the atmospheric corrosion behavior in Southern California and other well studied areas, the present study has clearly demonstrated the need for a more extensive California specific investigation of material damage due to acid deposition. The present study has also demonstrated the major aspects of the effects of acidic pollutants on corrosion of materials in Southern California. However, there are a number of important issues that still need clarification. The following suggestions cover the range from efforts that could be done better to new ideas for improving our ability to assess the damage caused by acid deposition in California.

Improved Damage Functions

Development of improved damage functions for acidic species will require the following:

Additional pollutant measurements. Monitoring of the criteria pollutants alone is insufficient. Additional measurements of all acidic species are necessary. This includes nitric acid vapor, acidic (and alkaline) species in airborne particulate matter, and organic acids as vapors and particles, in addition to improved measurements of sulfur dioxide. The frequency of particulate sampling should be increased from every sixth day to every third in order to get more precise estimates of quarterly averages.

Additional meteorological measurements. Solar radiation intensity in the visible and ultraviolet are required for estimation of damage functions for paint. A 30-meter meteorological tower instrumented for making estimates of momentum, moisture and heat flux to the surface would be highly desirable. Reliable relative humidity measurements are an absolute necessity, and an on-site recording rain gauge is desirable.

RECOMMENDATIONS FOR FUTURE RESEARCH (continued)

Improved damage measurements for painted surfaces. Weight loss measurements should be complimented with long term spectrophotometric measures of fading. Quantitative measures of cracking and peeling of paint on wood are needed. The paints to be studied should be applied to zinc and ACRMS for continuous monitoring of the coating properties and additional information such as water uptake audits fluctuation with the diurnal cycle.

Exposure Periods

The results of the present project have demonstrated very pronounced seasonal effects on corrosion rates for the metals (galvanized steel, nickel and aluminum) as well as for the nonmetals (paint and nylon). In any further field tests these results should be considered in the planning of the exposure schedule. For the three sites in Southern California, samples should be exposed each year in May and in November for 6-month and 12-month periods to compare the effects of the atmospheric conditions during the smog season and the winter time. Additional samples should be started in May and November for longer exposure times between one and five years.

Atmospheric Corrosion Rate Monitors (ACRM)

Much useful qualitative information has been obtained with the ACRMS which have the important advantage that the corrosion behavior is monitored continuously. Since a data point is determined every ten minutes during the entire test period, it is in principle possible to follow even short episodes of acid rain, dew or fog and determine the relationships between the corrosion rate information provided by the ACRMs and the atmospheric data. In the present project, this analysis could not be performed due to budget and time restraints and the emphasis on the determination of damage functions. A statistical analysis based on daily averages of the ACRM data has shown in most cases only weak correlations between these daily averages and the weight

RECOMMENDATIONS FOR FUTURE RESEARCH (continued)

loss data which represent averages over three, six or twelve months. The corrosion rates determined with the nickel sensor facing the sky showed the best correlation with weight loss. A much more detailed analysis of the ACRM data on a finer time scale and statistical analysis with equally spaced atmospheric data is necessary. The results of such an analysis would greatly improve our understanding of basic phenomena in atmospheric corrosion reactions.

Laboratory Studies

In the laboratory studies carried out in this project the effects of single pollutants such as SO_2 , NO_2 and O_3 and their combinations on the corrosion behavior of the test materials have been determined. In addition, the effects of HNO_3 aerosol of two concentrations and two flow rates have been determined. The results of a statistical analysis of the field test data have suggested that corrosion rates are higher in the summer than in the winter because of the corrosive nature of the products of photochemical oxidation reactions which occur in the summer. In order to determine in more detail the role of the individual species involved in these reactions and to detect synergistic and/or antagonistic effects, it is necessary to carry out additional laboratory studies in smog chambers. Such smog chambers are available in the Rancho Los Amigos Laboratories of the School of Medicine of USC. It is also necessary to determine the reaction mechanism(s) by which the reaction products of photochemical reactions cause damage to metals and non-metals such as nylon which have very similar seasonal variations.

1.0 INTRODUCTION

The Kapiloff Acid Deposition Act of 1982 (California Health and Safety Code, Section 39010.5, 39010.6, 39900 et seq.) requires the California Air Resources Board (CARB) to assess the economic impact of acid deposition upon materials as part of a comprehensive research program to determine the nature, extent and potential effects of acid deposition in California. However, before this can be accomplished, the material damage must be quantified. The National Acid Precipitation Assessment Program (NAPAP) (see: NAPAP's 1983 Annual Report; and NAPAP's Project List produced by Oak Ridge National Laboratories, March 1984) has recently sponsored research which will help in quantifying such damage to man-made and natural materials in the eastern United States. However, major uncertainties remain in understanding the specific role played by acid deposition constituents in materials deterioration. The major objective of the first phase of the California Air Resources Board's research program is to investigate this specific role in California by sponsoring research which gives particular attention to dry deposition, fogs, mist and dew.

Field exposure and laboratory chamber experiments to quantify were conducted in joint projects between Combustion Engineering Environmental's Environmental Monitoring and Services, Inc. (EMSI), Rockwell International Science Center (RISC), and the University of Southern California (USC). These projects were funded by CARB contracts A4-110-32 and A5-137-32, and concluded in 1988. A related project to specifically determine the role of acid fog in materials damage (CARB Contract A5-138-32) ran during the same time and is reported separately.

The objectives of this study of acid deposition damage to materials were:

- o To determine the damage rate of selected materials in Southern California as a function of acid deposition constituents;

- o To determine the contribution of natural weathering to the overall damage rate to these materials, and
- o To determine the synergistic, antagonistic, and additive effects of multiple ambient pollutants on materials, and express these effects as a damage function.

These three objectives were achieved through analysis of damage measurement data obtained from exposure of selected material specimens at three field sites in Southern California, one background site at Salinas in Central California, and in a laboratory test chamber with controlled atmospheres.

Southern California was chosen as the area of field measurements because it is the area where acid deposition material damage is considered highest due to elevated atmospheric pollution and large quantities of materials exposed. Specific materials were selected for their economic value and their vulnerability to both acid deposition damage and specific acid deposition components. Field exposure sites were colocated at CARB monitoring stations for comparison with monitored aerometric parameters. In addition, continuous atmospheric corrosion rates and periodic daily nitric acid samples were measured. Field sites were selected on the basis of high levels of specific acid deposition components. A background site was chosen for low levels of acid deposition components and otherwise similar ambient conditions to the polluted sites. Measurements at a background site provided an estimate of natural weathering and thereby helped assess the incremental damage due to acid deposition. The laboratory chamber tests determined the synergistic, antagonistic, and additive effects of multiple pollutants. Field exposure times ranged from 3 to 15 months with overlapping intermediate intervals to determine seasonal variations in damage rates.

2.0 PROJECT DESIGN

Several pollutants are generally simultaneously present in the atmosphere and their deposition may damage materials alone, additively, antagonistically, or synergistically. The deposition and attack of pollutants on objects are affected by several atmospheric factors such as local winds, temperature, sunlight, precipitation, relative humidity, fog, dew, sample orientation, etc., as well as by ambient pollutant concentrations. In addition, atmospheric corrosion of materials is an intermittent process occurring mainly during periods of surface wetness, and is accelerated in the presence of acidic pollutants. This is particularly important to recognize in Southern California, where precipitation is significant only during a brief rainy season; moisture condensation (dew) and fog are probably the main factors causing surface wetness. The rate and extent of materials damage depend on the reactivity of the materials and the corrosivity of the pollutants that deposit on their surface. For example, nylon is easily damaged by nitric acid, whereas damage to aluminum is slowed by the formation of a protective film as its corrosion product. Multi-component materials such as paint are affected according to the reactivity of their components. For example, calcium carbonate, used as an extender, is readily attacked by acids. Also, the dimensions of a material may change due to corrosion or corrosion products resulting in stresses to the material. For example, the rusting of reinforcing steel may cause concrete to crack. Thus, materials damage in the ambient atmosphere is affected by multiple factors.

Our approach to obtaining relationships between damage rate and acidic air pollutants as well as other atmospheric factors was to pursue a comprehensive experimental investigation involving field and laboratory exposure. The details of the program design are given in this section. The program was designed to take advantage of the best methods available to us and to answer the objectives of the program.

The project design addresses the experimental and design considerations involved in the selection of field sites, materials for damage quantification, damage measurement and field and laboratory exposure test protocols. Details of the procedures are given in the Appendix.

This report combines two very closely related programs under the two CARB contracts (A4-110-32 and A5-137-32). The second contract expanded and extended the initial program. The experimental design of the second program is based on and compatible with the initial program which used five materials. The field exposure period began in February and March 1986 and ended in July 1987; however, the second program maintained continued exposure of a set of four materials from the initial five and added four other materials. The second project field exposure program began in July 1987 and ended in July 1988. Both programs shared the same fundamental design considerations as described below.

2.1 MATERIALS SELECTION

The choice of specific materials was based primarily on the economic value of damage to materials susceptible to acid deposition damage. In the real world, only a few materials account for the major costs of damage (1). The economics of materials damage is affected by several factors:

1. Susceptibility to damage;
2. Extent of usage;
3. Cost of products in-situ (including material, manufacturing, and placement costs); and
4. Maintenance, repair and replacement costs.

For example, zinc is relatively inexpensive, but because of its widespread use for galvanizing steel, the economic loss due to damaged zinc can be significant. Similarly, the material cost of paint or concrete is small, but their use is widespread and in-situ and

replacement costs are high because of large labor expense. Hence, their damage is also economically significant.

Using this approach, Salmon (1) has comprehensively studied and ranked materials in the United States according to the economic loss resulting from their damage. This list is presented in Table 2-1, where typical uses and products are also given. The high ranking materials in Table 2-1 have also been identified as significantly susceptible to acid damage by Yocom and Baer (2). This information formed the starting point for material selection.

The economic value of material damage was adjusted to reflect current California usage on the basis of another CARB sponsored study. Secondary considerations for material selection included current, extensively used mitigation measures such as antioxidants in rubber products. Field exposure time limitations, specimen size and damage measurement properties were also considered. Selection of materials was discussed among project participants and CARB personnel and made by joint agreement.

The following materials were chosen:

A. Initial Program (first 15 months)

1. Zinc as galvanized steel
2. Nickel
3. Flat latex exterior house paint with carbonate extender
4. Flat latex exterior house paint without carbonate extender
5. Concrete as commercial concrete brick

B. Expanded/Extended Program (additional 12 months)

1. Zinc as galvanized steel
2. Nickel

TABLE 2-1. RANKING OF MATERIALS BY ECONOMIC LOSSES DUE TO AIR POLLUTION DAMAGE AND SOILING *

<u>Rank</u>	<u>Materials</u>	<u>Typical Products</u>
1	Paint	Industrial, household, automotive
2	Zinc	Galvanized products
3	Fibers	Cloth, garments, canvas
4	Cement & Concrete	Stucco, freeways
5	Nickel	Plated steel, automotive trim
6	Rubber	Tires
7	Tin	Brass products
8	Plastics	Consumer products
9	Aluminum	Window frames, electrical cable
10	Copper	Electrical cables, decorative roofs
11	Carbon steel	Industrial structures
12	Building brick	
13	Paper	
14	Leather	
15	Wood	House siding
16	Building stone	
17	Brass and bronze	
18	Magnesium	
19	Alloy steel	Automotive products, bridges
20	Bituminous materials	
21	Gray iron	Railing
22	Stainless steel	
23	Clay pipe	Drains
24	Malleable iron	
25	Chromium	Automotive trim
26	Silver	
27	Gold	
28	Glass	Windows, building exteriors
29	Lead	
30	Molybdenum	
31	Refractory ceramics	
32	Carbon and graphite	

*From Salmon (1)

3. Flat latex exterior house paint with carbonate extender
4. Flat latex exterior house paint without carbonate extender
5. Flat latex exterior house paint without carbonate extender on wood
6. Aluminum
7. Nylon fabric
8. Polyethylene plastic

Galvanized Steel

Zinc is primarily used in the production of galvanized iron and steel. Although zinc is relatively inexpensive, it is readily susceptible to acid damage with zinc damage ranked second in economic loss by Salmon (1). Zinc is also one of the most common materials used internationally for corrosion damage field studies (3) and is one of the materials used in the world-wide study by the International Standards Organization (ISO). Thus, zinc damage is a useful parameter for comparing Southern California with other studied regions. Galvanized steel was selected to quantify damage to zinc because it is the application of zinc most economically important with regard to acid deposition damage. Commercially available galvanized steel is usually passivated by a chromate dip to enhance its early weathering properties. However, for this short duration study, non-passivated (chromate-free) galvanized steel was selected so as to avoid the inhibiting effect of chromate in the measurement of zinc damage. Zinc atmospheric corrosion rate monitors (ACRM) were also used and provided corroborative data between the monitors and galvanized steel samples.

Nickel

Nickel is economically important (see Table 2-1), because of its high cost and its use in electroplating of metals. Nickel is also sensitive to damage by nitric acid, but is relatively resistant to

damage by sulfuric acid. Since zinc and nickel have different corrosion resistance in exposure to H_2SO_4 and HNO_3 , the corrosion data for these two materials might provide some information on the relative damage effects of H_2SO_4 and HNO_3 . To quantify damage to nickel, commercial grade nickel (Nickel 200, 95% pure) was selected. Nickel and zinc are the two metals used in the sensors for the atmospheric corrosion rate monitor (ACRM), thus nickel corrosion rate data can be compared to the nickel specimen corrosion damage data.

Exterior House Paint

Paints, as a class, are ranked highest for economic damage from air pollution and acid deposition. Among exterior paints, two types, automotive finishes and pre-painted enamels, were not considered. Both have long design lives so that atmospheric acid damage is not significant. Exterior house paint was chosen as the best category of paint for an outdoor study. Vinyl acrylic latex paints are among the most widely used house paints in California and, therefore, were selected for this study.

Vinyl acrylic resins, the vehicle in the paint, are resistant to acid damage. It is the other ingredients, such as calcium carbonate, zinc oxide, etc., that are susceptible to acid damage. Although the trend is toward not using calcium carbonate because of its susceptibility to acids (4), it is still, at present, widely used in paints. Thus, two of the commonly used brands of vinyl acrylic latex paints, one with and one without carbonate extenders, were selected for this study. They were both a similar off-white color (Navajo White).

In the initial program, both paints were applied to stainless steel, a nonreactive substrate suitable for paint weight loss measurement. This enables evaluation of the reaction of carbonate in the paint with pollutants by weight loss without confounding factors due to substrate damage.

In the expanded/extended program, low carbonate paint applied to a wood substrate was added to evaluate appearance damage to painted wood as a function of acid deposition variables. Wood is a common "real world" substrate for this type of paint. Wood was not used in the initial program because weight loss from wood is greater and more variable than paint weight loss. However, based on experience gained in the first year of the project, it was possible to quantify appearance damage and thus overcome the limitations of wood for weight loss studies.

Concrete

Cement and concrete are ranked 4th by Salmon (1) and are extensively used in many forms in Southern California. To quantify damage to concrete, samples were cut from commercially available concrete bricks. Concrete bricks are one of the concrete products used in outdoor construction and present a more convenient and uniform sample than cast in-situ concrete samples. The concrete bricks were made from equal parts Portland Cement, quarried sand, and gravel aggregate. This is a common type of concrete brick.

Aluminum

Aluminum is ranked 9th by Salmon (1). Aluminum is extensively used in Southern California for outdoor building material. The Upland site, for example, is within a mobile home community with hundreds of aluminum homes. Aluminum was a material specified by CARB; the type selected was an 1100 series H-14 aluminum with a thickness of 0.127 centimeter (0.05 inch).

Nylon

Fibers for cloth are ranked 3rd by Salmon (1). Nylon fabric is economically important in clothing and fabric used outdoors. A non-treated filament used for outer shells of garments was the type chosen.

Nylon is also used in hardware and as a component of tires. Although the extensive outdoor use of nylon is debatable, this material was selected per requirements of CARB.

High Density Polyethylene

Plastics are ranked eighth by Salmon (1) and are extensively used for outdoor materials in Southern California. For example, High Density Polyethylene is used as wear guard material providing a soft and protective surface. Plastics are generally resistant to acid damage, but High Density Polyethylene (HDPE) was specified by CARB as one of the materials to be studied.

Summary

Eight out of the top ten materials listed by Salmon (1) were chosen for study. Rubber (ranked sixth) was not selected because of antioxidants now commonly added to its products. The antioxidants reduce ozone damage which is the dominant air pollutant damaging agent for rubber. Also, in-service damage to automotive tires, the major rubber product, is so severe that it may not be possible to isolate acid damage. Tin (ranked seventh) was not selected because of its low usage in Southern California. The usage of tin in general has probably been reduced significantly since Salmon (1) ranked it. Tin is more commonly used as an alloying agent and damage measurement for alloys is complicated because of their varying properties.

2.2 MEASUREMENT OF DAMAGE

The determination of the relationship between material damage rates and atmospheric factors requires the simultaneous measurement of damage rates and either direct measurements of deposition flux and surface wetness or, at least, the measurement of factors affecting them such as air pollution concentrations. Alternatively, the combined effects of various atmospheric factors contributing to materials damage can be

determined by a single atmospheric corrosivity index and material damage rates correlated with it. Atmospheric measurements and field and laboratory tests are addressed in later sections.

The mechanisms and causes of materials damage must be understood before a program can be designed to evaluate the effects of acid deposition on materials. Materials damage may be divided into three main mechanisms:

1. Direct chemical reaction between the pollutant and material.
2. Indirect chemical attack where the pollutant is first absorbed onto the material surface. Damage occurs by transformation of the pollutant followed by chemical reaction, e.g., the transformation of SO_2 to H_2SO_4 , which then reacts with the material.
3. Electrochemical corrosion due to the formation of numerous small electrochemical cells on metal surfaces. Corrosion occurs when current flows between such cells in the presence of an ionically conductive moisture film.

Whereas direct and indirect chemical attack mainly affect non-metals (cement, stone, etc.), atmospheric corrosion of metals is of electrochemical nature.

Materials damage is evidenced by surface erosion and loss of material (stone, metals), increased stress due to change in dimensions (stone, metals, cement), cracking (leather, rubber), discoloration (paints, dyes), and loss of strength (fibers, rubber). Loss of material may itself contribute to the loss of strength in products and structures.

Damage to materials can thus be quantified by measuring changes in physical properties such as the degradation of strength, weight loss of material, surface properties, physical properties of the material after exposure to specified conditions and time, or by monitoring the electrochemical corrosion process. Both the physical and electrochemical approaches were used in this project.

Physical Property Measurements

Quantifying damage by physical property degradation requires measurement of materials before and after exposure. The difference in measurement results represents the damage. In this project, the physical properties used were weight (to indicate loss of material) and strength. Weight loss was used to quantify damage to the metals and painted stainless steel, and was determined by exposing pre-weighed samples, and post-weighing the exposed samples after removal of corrosion products by appropriate means. The weight loss, when corrected for blanks (the weight loss of samples with zero exposure time, but otherwise processed identically) represents material damage. In this program, damage to galvanized steel, nickel, aluminum, and paints on stainless steel (S.S.) was determined by weight loss (weight loss for concrete was also attempted but proved unsuccessful). The sample size was 15.24 x 10.16 cm (6 x 4 in) from gauge sheet stock (for paint, 15.24 x 10.16 cm (6 x 4 in) S.S. substrate was used). This size was selected as large enough to minimize corrosion effects along edges and at the same time to hold the total weight under 200 g so that typical weight losses (10-100 mg) could be measured by precision balances within ± 0.1 mg. Weight loss estimates were made from duplicate samples. The details of weight loss measurements for specific materials are given in the Appendix.

Strength loss was used to quantify damage to nylon. The loss in breaking strength to nylon samples after exposure was compared to the strength of the unexposed sample. The breaking strength of the fabric was measured by a raveled strip test. Raveled 2.54 cm (1 in) strips were cut from larger pieces that were exposed (or unexposed control samples). This is discussed in detail in the Appendix.

Another physical property measurement attempted but unsuccessful was the electromechanical impedance measurement on paints applied to stainless steel. The paints were too porous even before exposure to yield meaningful results.

Electrochemical Monitoring of Atmospheric Corrosion Rates and Time-of-Wetness

Our present knowledge of atmospheric corrosion clearly shows that no atmospheric exposure test can be complete without a continuous record of the time-of-wetness and corrosivity of the microclimate at the test site. These can be obtained with electrochemical sensors.

Since the atmospheric corrosion process for metals is electrochemical in nature, it is possible to determine corrosion damage by monitoring a metal's corrosion current. A continuous record of the corrosion rate is obtained in this manner, making it possible to establish correlations with atmospheric parameters and their changes. As a "by-product" of the electrochemical measurement, the time-of-wetness, t_w , is obtained indicating the fraction of the exposure time during which enough corrosive electrolyte and moisture are present on a metal surface to make corrosion possible.

The use of electrochemical sensors in studies of atmospheric corrosion has been pioneered in the U.S. by Mansfeld and co-workers (1977-1985) (5-9). The atmospheric corrosion monitor (ACM) was first used in an exposure study in St. Louis which was funded by the EPA (5). The design of an improved sensor - the Atmospheric Corrosion Rate Monitor (ACRM) - and its operation have been described in detail (9). The sensors are controlled by the atmospheric corrosion rate monitor data logger (ACRMDL), which also stores the data (7-9).

Two zinc and two nickel ACRMS were exposed at each test site. One sensor of each type faced skyward, the other faced the ground. The different orientation of the sensors was used to determine the effects of washing by rain, exposure to direct sunlight, and other factors on corrosion rates and on t_w . The data from the sensors were automatically logged using the ACRMDL and retrieved for analyses of time of wetness, corrosion rates and correlations with atmospheric data (8-11).

The quantity measured by the ACRM is the polarization resistance, R_p , which is inversely proportional to the corrosion current density i_{corr} :

$$R_p = \frac{B}{i_{corr}} \quad (\text{Eq. 2-1})$$

Application of Eq. 2-1 requires knowledge of the factor B, which depends on kinetic parameters (12). Since B can change with environmental conditions and with time and because its exact value is often unknown for a given application, a theoretical value of B=20 mV is often used. The electrochemical measurement carried out here is basically a determination of R_p . Integration of the R_p^{-1} vs. time curves for a field or laboratory test gives the integrated corrosion loss in units such as sec/ohm for any desired time period. With the assumption for B discussed above, and Faraday's law, a corrosion rate is calculated.

The time-of-wetness, t_w , was also obtained from the ACRM data and was called the corrosion time, t_{corr} , to distinguish it from the time-of-wetness which is usually estimated as the time for which RH > 80% and T > 0°C.

Appearance Measurement

The degradation of the appearance of paints is another major consequence of acid damage. For example, several types of changes can affect a paint film's appearance (13):

- o Pigment fading or darkening
- o Gloss increase or decrease
- o Surface chalking (white or chromatic)
- o Dirt accumulation

- o Bronzing
- o Vehicle yellowing
- o Internal separation of pigment from binder

All these changes affect the perceived color and appearance of the paint film.

If each of these types of appearance changes were to occur singly, the visual effect of each would be readily distinguishable but, generally, several effects occur simultaneously. Although that fact may be readily apparent, the actual magnitude of the effect of each change and its importance on the total perceived color difference are not. Visual examination primarily reveals the cumulative effects of all changes that have occurred.

Although the measurement of the color change by either a tristimulus colorimeter or a spectrophotometer provides more objective information concerning the observed change than subjective visual evaluations alone, the interpretation of the type of change that contributes to the measurement results is not obvious. An accurate and sensitive method for spectrophotometric measurement of appearance degradation has been developed (14). Using spectrophotometric data, before and after exposure, and a computer program, an experienced technologist can evaluate the damage to paints. Specifically, changes in pigment color (or vehicle color), changes in surface reflectance (such as change in gloss or bronzing), as well as changes correlating with total visual evaluation (the integrated differences of all changes) can be measured. Since paints are one of the most important materials, the appearance measurements were used to evaluate damage to a selected number of paint samples.

2.3 FIELD EXPOSURE

The previous section discussed the measurement of damage caused by atmospheric corrosion. To formulate damage functions, damage rates are

needed over pre-determined exposure periods, either in the field or in the laboratory. The experimental procedures for field exposure are addressed in this section, those for laboratory exposure are addressed in Section 2.4.

Site Selection

Site selection is one of the most important aspects of the field exposure operations. The goal of site selection is to provide sites with sufficiently different local environments such that the effects of specific pollutants on materials damage can be discerned. Two sites with local environments identical in all respects except for one pollutant were considered. In the absence of synergism, the difference in materials damage at the two sites can, therefore, be considered to be due to the difference in that pollutant at the two sites.

As proposed by CARB at a meeting in Sacramento in August 1985, the following site location constraints were adopted:

1. Colocation of materials damage sites with CARB's HNO_3 program sites as far as practical.
2. Limitation of exposure sites to the South Coast Air Basin.

Since four sites were funded, quantifying the effect of only a few pollutants was attempted. Since the main acidic pollutants are HNO_3 , NO_2 and SO_2 , we have selected the sites primarily on the basis of these three species although the SO_2 concentrations in Southern California are generally low. Because of these limitations, other atmospheric parameters such as fog have not been considered in this program. However, acid fog is addressed in a related project funded by ARB which is reported separately (15). The selected sites and their pollution data are listed in Table 2-2 and a map is shown in Figure 2-1. Since HNO_3 is being measured for CARB by another contractor, we have limited our site choices to the same sites as far as practical. We also independently monitored HNO_3 at all sites. All sites have been collocated with sites in CARB's air monitoring network so that air

TABLE 2-2. ANNUAL SITE POLLUTION LEVELS (1982 - 1984 Average)

<u>Site</u>	<u>NO₂</u> <u>ppb</u>	<u>SO₂</u> <u>ppb</u>	<u>NO₃⁻</u> <u>ug/m³</u>	<u>SO₄⁼</u> <u>ug/m³</u>	<u>O₃</u> <u>ppb</u>
Long Beach	48.8	9.8	11.45*	9.40	15.3
Burbank	57.8	5.2	---	---	26.0
Upland	43.4**	2.1**	17.59*	9.05*	31.7
Salinas	12.4	0.20	3.96	3.75	20.0

* One year data

** Two year data; 1981-1982

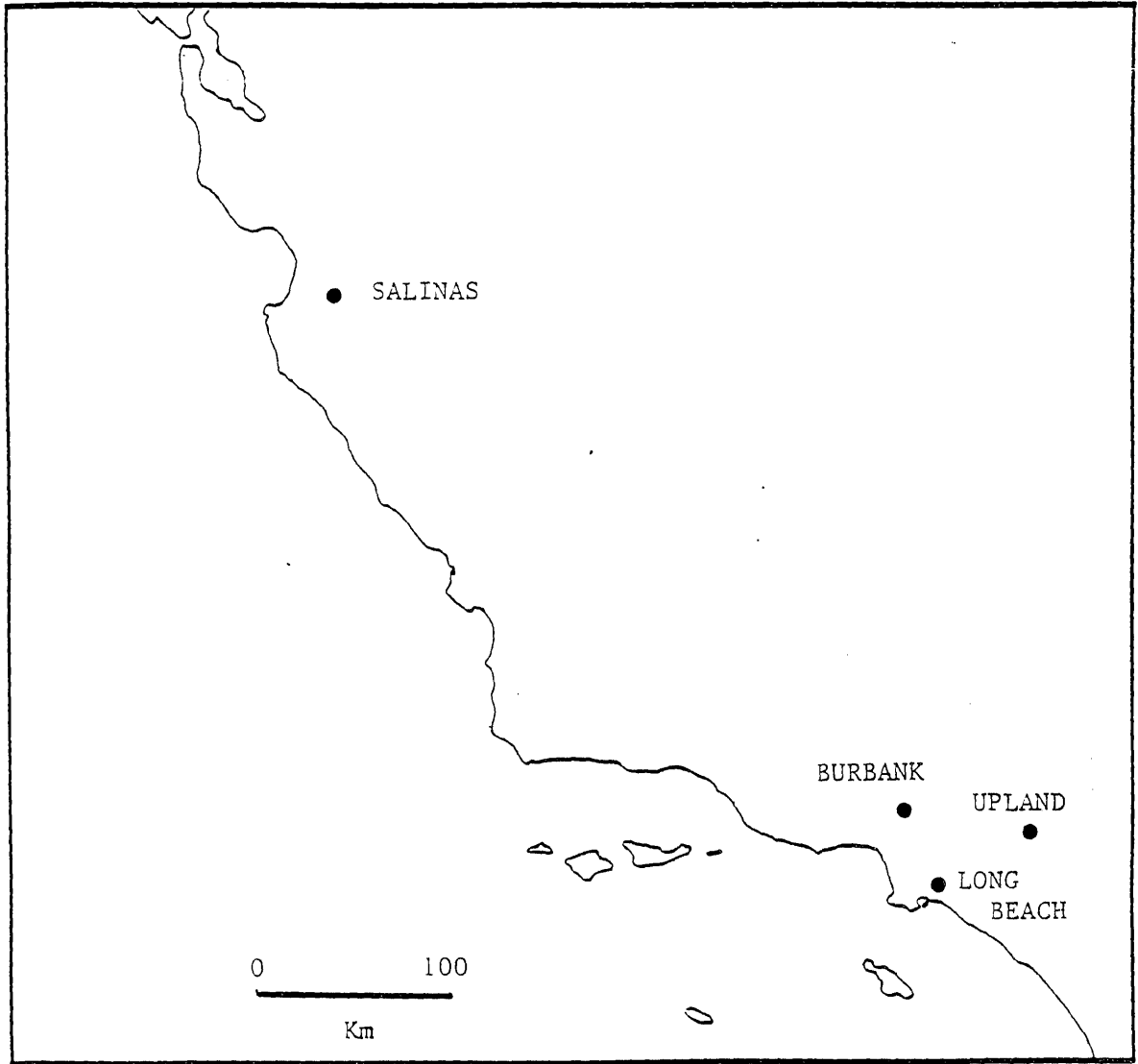


FIGURE 2-1. SITE LOCATION MAP

pollutant data are available from CARB for our data analyses.

Although O_3 is not an acidic pollutant, ozone concentrations are listed in Table 2-2, since synergistic damage effect due to O_3 is expected. Further, O_3 is believed to be a good surrogate for HNO_3 . The NO_2 level at Burbank is about one-fifth greater than in Long Beach, whereas the SO_2 level at Burbank is only half of that in Long Beach. The two sites were, therefore, selected to indicate the effects of these two pollutants. Upland has moderate SO_2 and NO_2 levels relative to Burbank and Long Beach. NO_2 is about 12% lower and SO_2 is only 20% of that in Long Beach. Being at the extremity of the basin, high HNO_3 levels were anticipated for Upland. Thus, Upland was selected to identify predominantly nitric acid damage.

For the low pollutant site, it was decided to look outside the basin, since all sites within the basin experience relatively high pollutant levels. The monitoring station in Salinas known as Salinas II (Salinas) was chosen. The NO_2 levels are about one quarter and SO_2 levels only a fraction of those at Burbank or Long Beach. It should be noted that Salinas is not a part of CARB's nitric acid program. Although Salinas is in Central California the climatology is similar to the Southern California sites.

Salinas, Burbank, Long Beach and Upland all have coastal or coastal valley Mediterranean climate. As seen in Table 2-3, Salinas' annual average climate data are similar to the other sites. When the annual average temperatures for all 4 sites are in turn averaged, the mean value is $16.9^{\circ}C$ ($62.5^{\circ}F$) with a maximum variance between sites of $2.6^{\circ}C$ ($4.6^{\circ}F$). When the annual average rainfalls for all 4 sites are in turn averaged, the mean value is 35.56 cm (14.00 in) with a maximum variation between sites of 18%. These temperature and rainfall differences are small enough to have little expected effect on the material damage rates.

TABLE 2-3. AVERAGE ANNUAL CLIMATIC DATA FROM STATIONS REPRESENTING THE FIELD SITES.

<u>Stations</u>	<u>Annual Average Temperature (°C)</u>	<u>Annual Average Precipitation(cm)</u>
Salinas (Airport)	14.4 (57.9°F)	33.04 (13.01 in.)
Long Beach (Airport)	17.7 (63.9°F)	29.31 (11.54 in.)
Burbank (Valley Pump Plant)	17.7 (63.9°F)	40.08 (15.78 in.)
Upland (San Bernardino County Hospital)	17.9 (64.2°F)	39.83 (15.68 in.)
Average	16.9 (62.5°F)	35.56 (14.00 in.)

Source: Climatological Data Annual Summary
California 1987, Vol. 91, No. 13

The primary issue in selecting field exposure periods was the resolution to differentiate seasonal differences. Seasonal differences in damage are caused by seasonal pollutant and climatic changes. Further, past evidence also suggested that the initial exposure conditions substantially affect the total corrosion over longer periods. This is especially true for zinc (5,6).

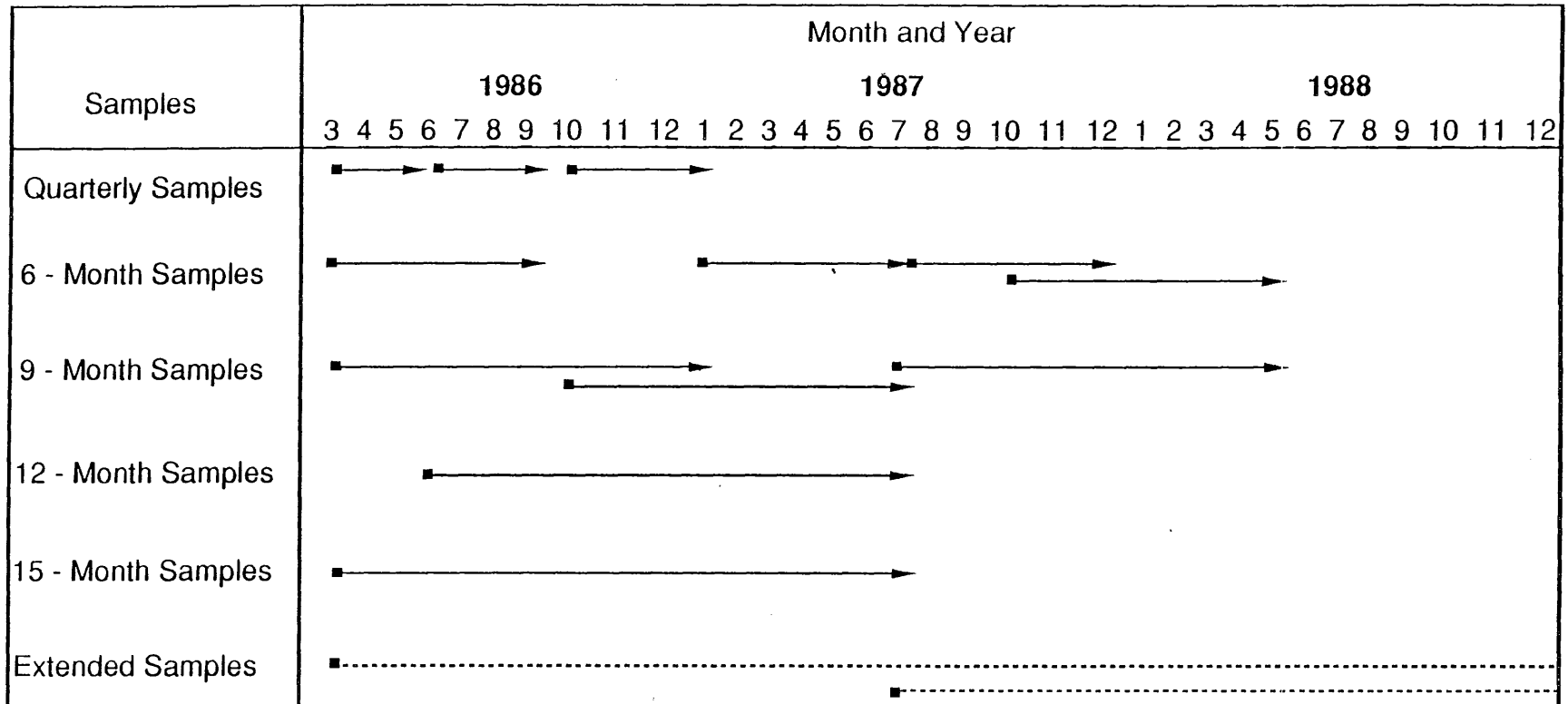
In this program, quarterly (3-month) exposure periods for the first year and 6-month exposure periods for the second year were selected to differentiate the seasonal effects. Although quarterly exposures are desirable, due to budget constraints this was possible only during the first year. However, in Southern California, there are only two predominant seasons - the dry warm season and the cool wet season. Therefore, relying on 6 month exposure resolution should be adequate to study seasonal effects.

To study longer term corrosion damage and to determine the effects of the initial exposure on total damage, 9 and 12 months and longer exposure periods were also selected commencing in different seasons. Figure 2-2 shows the details of the exposure sequence.

Duplicate samples for each exposure period were mounted per ASTM G50 on exposure racks inclined 30° to the horizontal and oriented so that the samples were facing south. The samples are held in place by porcelain insulator mounts so that galvanic corrosion between samples and mounting hardware was eliminated. A photograph of a rack at one site is shown in Figure 2-3a and a close up photograph showing specimens and mounting is shown in Figure 2-3b.

Aerometric Measurement

To quantify materials damage by damage functions requires simultaneously acquired damage and aerometric data for the micro-climate of the test site. To minimize duplication and effort, the majority of the required aerometric data was obtained from the CARB air monitoring



- → Exposure period
 ■ Exposures beyond this program

FIGURE 2-2. FIELD SAMPLE EXPOSURE SCHEDULE

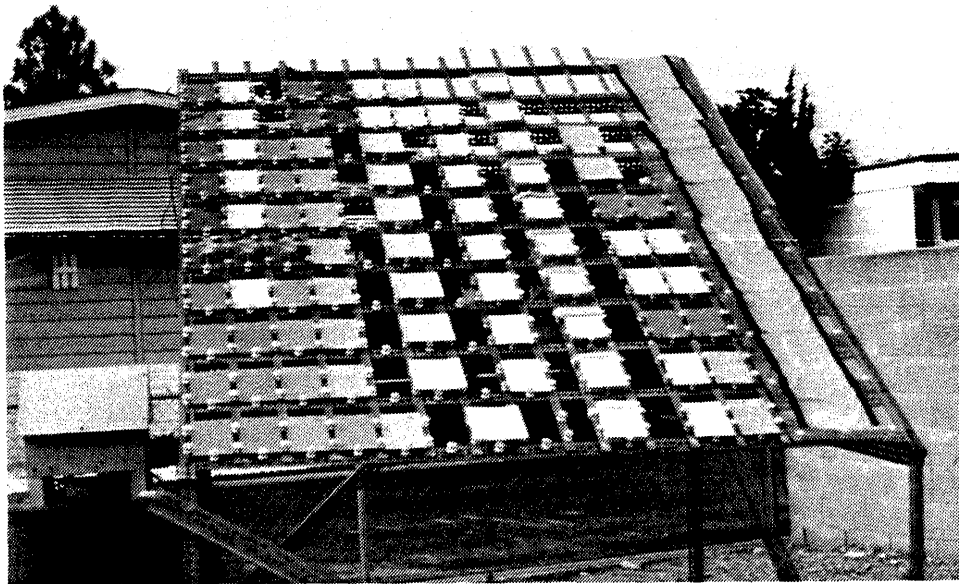


FIGURE 2-3a. FIELD SITE PHOTOGRAPH OF SPECIMEN RACK, UPLAND.

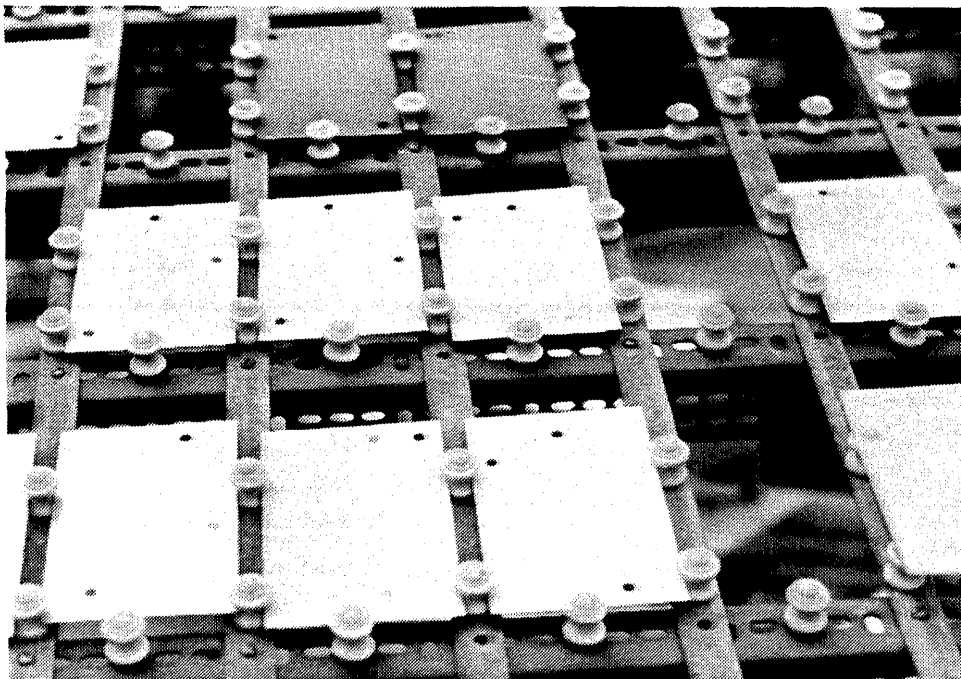


FIGURE 2-3b. CLOSE UP OF SPECIMEN RACK

stations at the selected sites where the exposure measurements were collected. The only variables of interest not available from the CARB sites were relative humidity (RH) and HNO_3 concentration. The ACRMDL has a built-in RH probe to provide continuous RH data at each site.

HNO_3 vapor was determined by the use of two-stage filter packs containing 37 mm Teflon and nylon filters. The Teflon filter, to remove particles, was upstream of the nylon filter. HNO_3 was captured by nylon filters which were then analyzed for nitrate. The filter packs were operated at 4 l/min. for 24 hours every sixth day. Longer periods are believed to run into filter loading problems (16).

2.4 LABORATORY EXPERIMENTS

In any field program, there are more variables than can be realistically measured. In our case, for example, there were more pollutants that are simultaneously present than were measured by CARB. In materials damage studies, a controlled laboratory exposure study provides damage due to specific pollutants or other conditions (fog), and the exposure itself is accelerated by simulated diurnal cycles and by elevated pollutant concentrations. In this program design, reliance was placed on laboratory exposure to provide information on the relative damage effects of several pollutants, singly and in combination. Such information was useful in deriving damage functions based on field data.

In the laboratory tests, specimens of the same materials exposed at the four field sites plus zinc and nickel ACRMs, were exposed to atmospheres of carefully controlled concentrations of pollutants for periods of 28 days/test. In each test a 6-hour cycle consisting of 1.5 hours at 16°C and 4.5 hours at 22°C was used. The cooling cycle was used to induce condensation on the sample surface. The test procedure will be described below, followed by the results obtained for the test coupons and the ACRMs.

Laboratory tests were run to investigate the effects of SO₂, NO₂, O₃ and their combinations. In addition, the effects of H₂SO₄ and HNO₃ were studied. Table 2-3 shows the test matrix in which SC denotes tests performed at the Rockwell International Science Center (see report for first contract (17) and USC denotes tests carried out at the Corrosion and Environmental Effects Laboratory (CEEL) at USC.

Test Procedure

The test coupons and coupons with ACRMs mounted to them were attached to the test chamber wall which can be cooled by circulating cold water outside the wall simulating diurnal condensation. Figure 2-4 shows a block diagram of the control instrumentation and the test chamber. The system is an improved version of that which was used in the first phase of this project at the Rockwell International Science Center (17). It was designed and built by Dwight Landis of ATEC, Agoura Hills, California, and includes the program control unit, the flow control unit, the test chamber with a temperature control bath, the aerosol generator, the monitoring devices for the pollutants and the ACRMDL.

Control Units

The program control unit (ChronTrol) controls the test at all times. It is able to provide up to 10 programs in four test conditions. In the tests for this study, three conditions were used: circuit 1 (22°C, RH = 80%), circuit 2 (16°C) and circuit 3 (aerosol). This program results in four 6-hour cycles per day as explained above. The flow of wet and dry air and pollutants (SO₂, NO₂) is controlled by four FC - 280 mass flow controllers (Tylan) with a maximum error of 1 ml/min. In all tests wet air, which was produced in the humidifier, and dry air were mixed to obtain RH = 80% at 22°C and a flow rate of 8 l/min. The SO₂ and NO₂ cylinder gases were obtained with a concentration of about

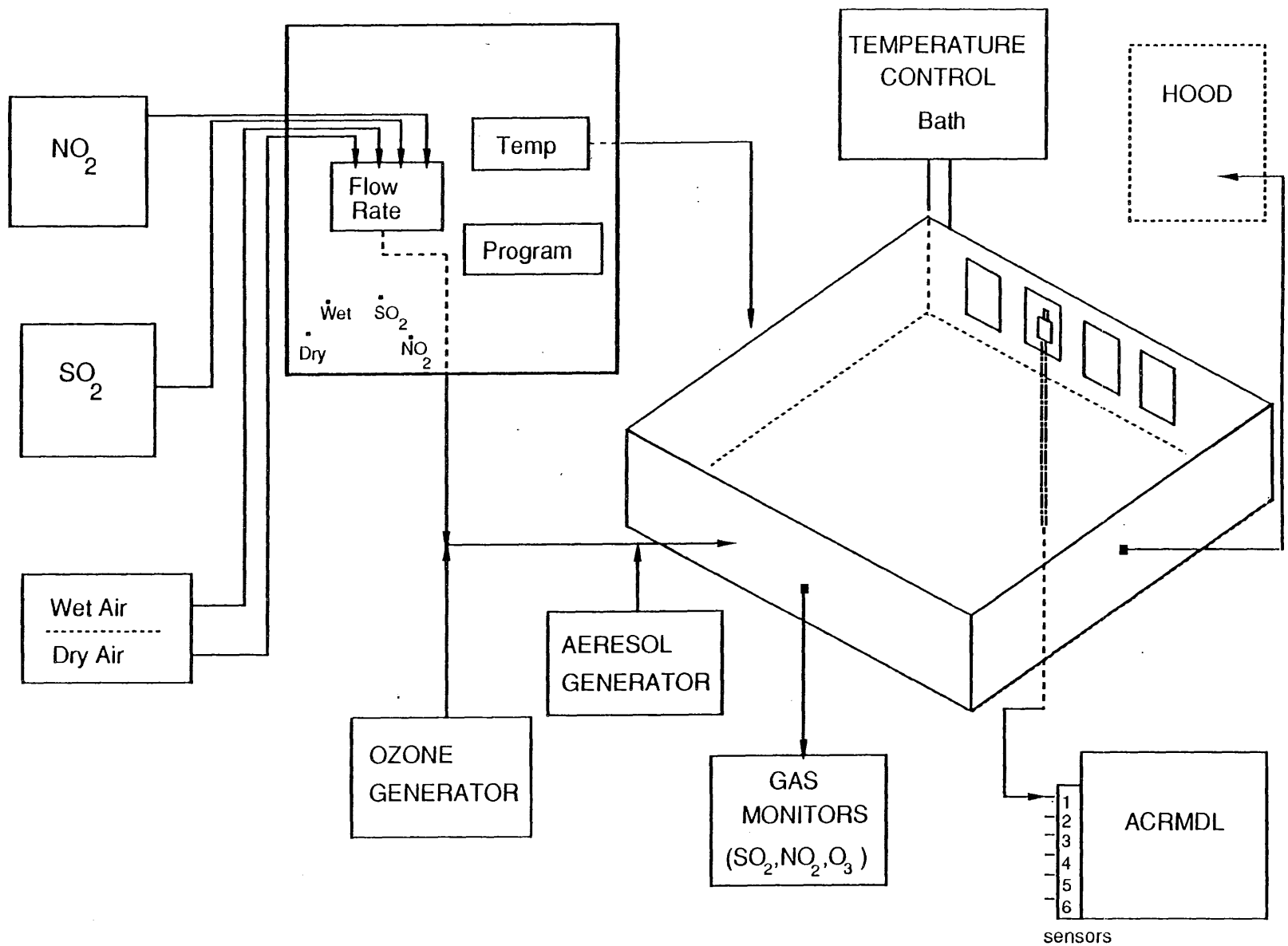


FIGURE 2-4. LABORATORY ACID DEPOSITION CHAMBER

480 ppm for SO₂ and 320 ppm for NO₂. An ozone generator was used to produce O₃, with the maximum concentration obtained 0.1 ppm.

The concentrations of SO₂ and NO₂ were monitored at the exit of the test chamber using equipment obtained from EMSI. The input concentrations were adjusted in preliminary tests to obtain the desired concentrations of 1.0 or 0.5 ppm at the exit of the chamber. The SO₂ concentration was monitored at the exit of the chamber using a Pulsed Fluorescent SO₂ analyzer (Monitor Labs Model 8850), NO₂ was monitored with an NO_x Analyzer (Monitor Labs Model 8440), and O₃ was monitored with an Ozone Concentration Analyzer (Dasibi Model 1003 AH). Pollutant concentrations were monitored at regular intervals and occasionally recorded as a function of time on a strip chart recorder.

The aerosol generator was a 500 cm³ micronebulizer. Aerosol was generated by nebulizing a 8 mM HNO₃ solution at a flow rate of 8 l/min. and introducing it into the test chamber. Nominal concentrations of 0.5 and 0.1 ppm were used.

The Test Chamber

The test chamber was a rectangular housing with a Teflon-coated interior. Samples were attached to the walls having room for four 10.2 cm x 15.2 cm coupons/per wall. On one coupon was mounted an ACRM. All inlets and outlets for gases and the ACRM leads were located at the bottom of the test chamber. A fan in the shape of a 3-blade propeller was used to ensure uniform distribution of the pollutants in the test chamber. The test sequence consisting of the 6-hour cooling/heating cycle was thermo-regulated by a TE-8J Tempette thermo-regulator in a Techne bath. The cover of the test cell was made of clear plastic which allowed visual observation of the samples during the test.

3.0 RESULTS AND DISCUSSIONS

Results from 24 months of exposure at the field sites and from 20 laboratory experiments are presented in this section. Quantification of the results by the derivation of damage functions is addressed in Section 4. As described in previous sections, damage to materials was differentiated by several methods. Of these, only weight loss, continuous electrochemical corrosion rate measurements, and strength loss for fabrics yielded useful data. The main discussion in this section is, therefore, devoted to these results.

3.1 FIELD MEASUREMENT

Damage data for the materials investigated in field exposure are discussed here; they are quantified by damage functions in Section 4.0. Data for galvanized steel, nickel and house paint on stainless steel are available for the period between April 1986 and March 1988. For aluminum, nylon, and polyethylene (HDPE), data are available for the period between November 1987 and March 1988. Damage was determined for exposure periods ranging from 3 months to 18 months.

3.1.1 Weight Loss Data

Weight loss was the damage measurement method used for galvanized steel, nickel, house paint, and aluminum. The weight loss data for those materials are discussed below.

3.1.1.1 Galvanized Steel

Figure 3-1 shows the weight loss data for the first set of galvanized steel at the four test sites. The first set of samples at Burbank was exposed in the last week of February 1986, while exposure at the other sites started in March. Several observations can be made by inspection of Figure 3-1. It can be seen that there was not much difference in weight loss at the four sites. At Upland the weight loss

GALVANIZED STEEL - FIRST SET

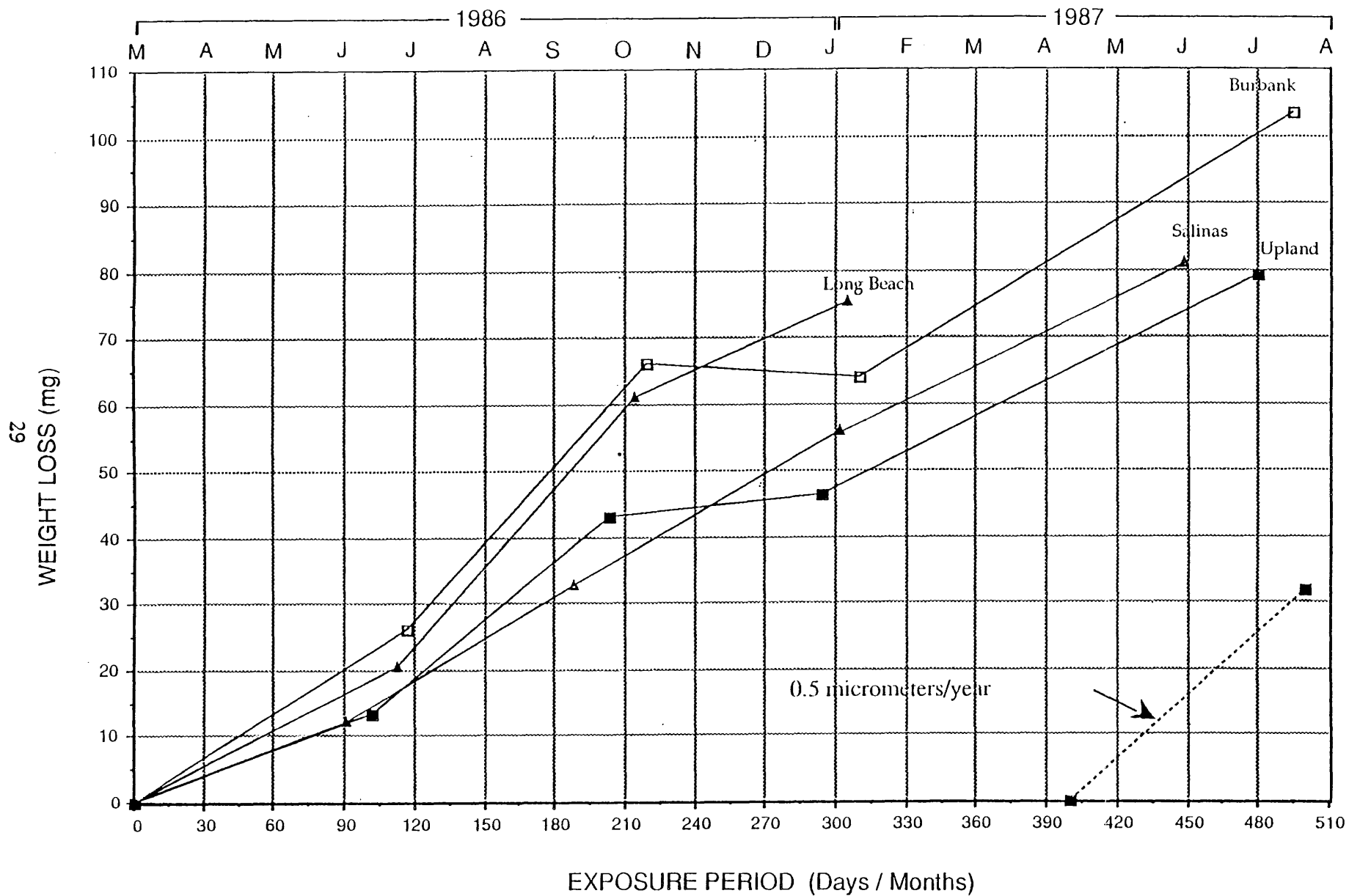


FIGURE 3-1. WEIGHT LOSS VS. TIME FOR GALVANIZED STEEL, FIRST SET

after one year was somewhat less than that at the "clean" site, Salinas. Corrosion rates were very low, amounting to less than 0.5 $\mu\text{m}/\text{year}$ which is typical of a rural site. For Burbank and Upland, the differential corrosion rate was very low for the time between October 1986 and January 1987. This can be seen in more detail in Figure 3-2 for Burbank, where the weight loss data were plotted for sets of samples with exposure beginning at different times in 1986 and 1987. By comparing the slope of the weight loss - time curves for the first three months, it became obvious that corrosion rates were similar for samples which were first exposed in February and June 1986, but much lower for first exposures in October 1986 and January 1987. The fifth set, which was exposed in July 1987, showed the highest corrosion rate. Corrosion rates for the sixth set, first exposed in October 1987, were very low for the first six months. The very low weight loss rates indicated by small slopes in the winter months were observed at all four test sites and for different sample sets.

3.1.1.2 Nickel

Figures 3-3 and 3-4 show the weight loss data for nickel. In this case, corrosion damage at the site in Salinas was much lower than at the other sites, with damage at Burbank and Long Beach appearing nearly the same. Corrosion rates were also very low for nickel and decreased for the winter months as shown in Figure 3-4 for the six sets first exposed between February 1986 and October 1987 at Burbank. Similar results were obtained at the other three sites with weight loss data between 0.07 mg/day for Upland and 0.12 mg/day at Long Beach.

3.1.1.3 House Paint

The weight loss data plot (Figure 3-5) for paint containing the carbonate extender showed the same trends as those for nickel (Figure 3-3) with similar data for Burbank and Long Beach and the lowest value for Salinas. The seasonal effects were less pronounced in the cases illustrated in Figures 3-3 and 3-5. For the paint without carbonate

GALVANIZED STEEL / BURBANK

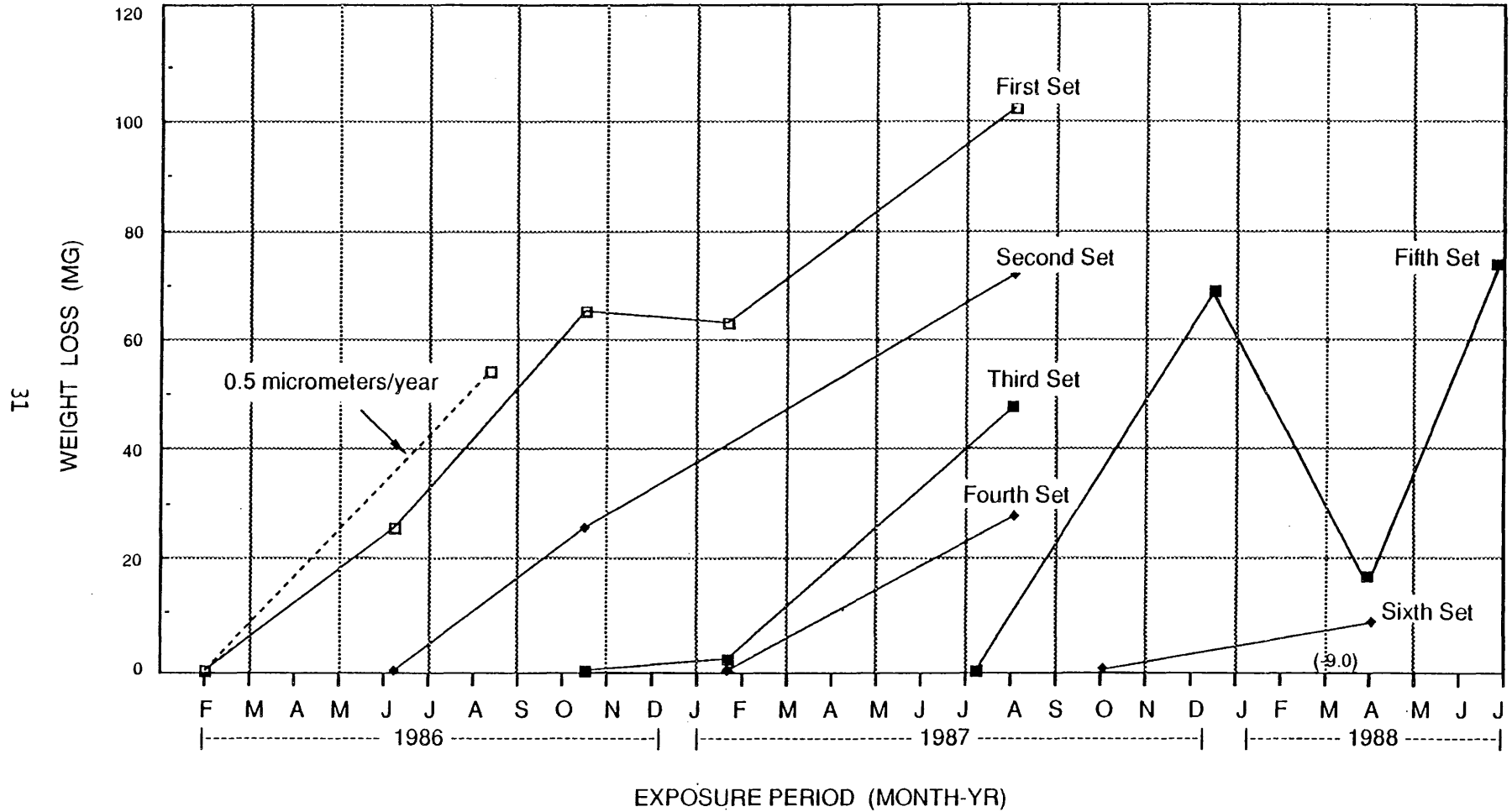


FIGURE 3-2. WEIGHT LOSS VS. TIME FOR GALVANIZED STEEL, BURBANK SITE

NICKEL- FIRST SET

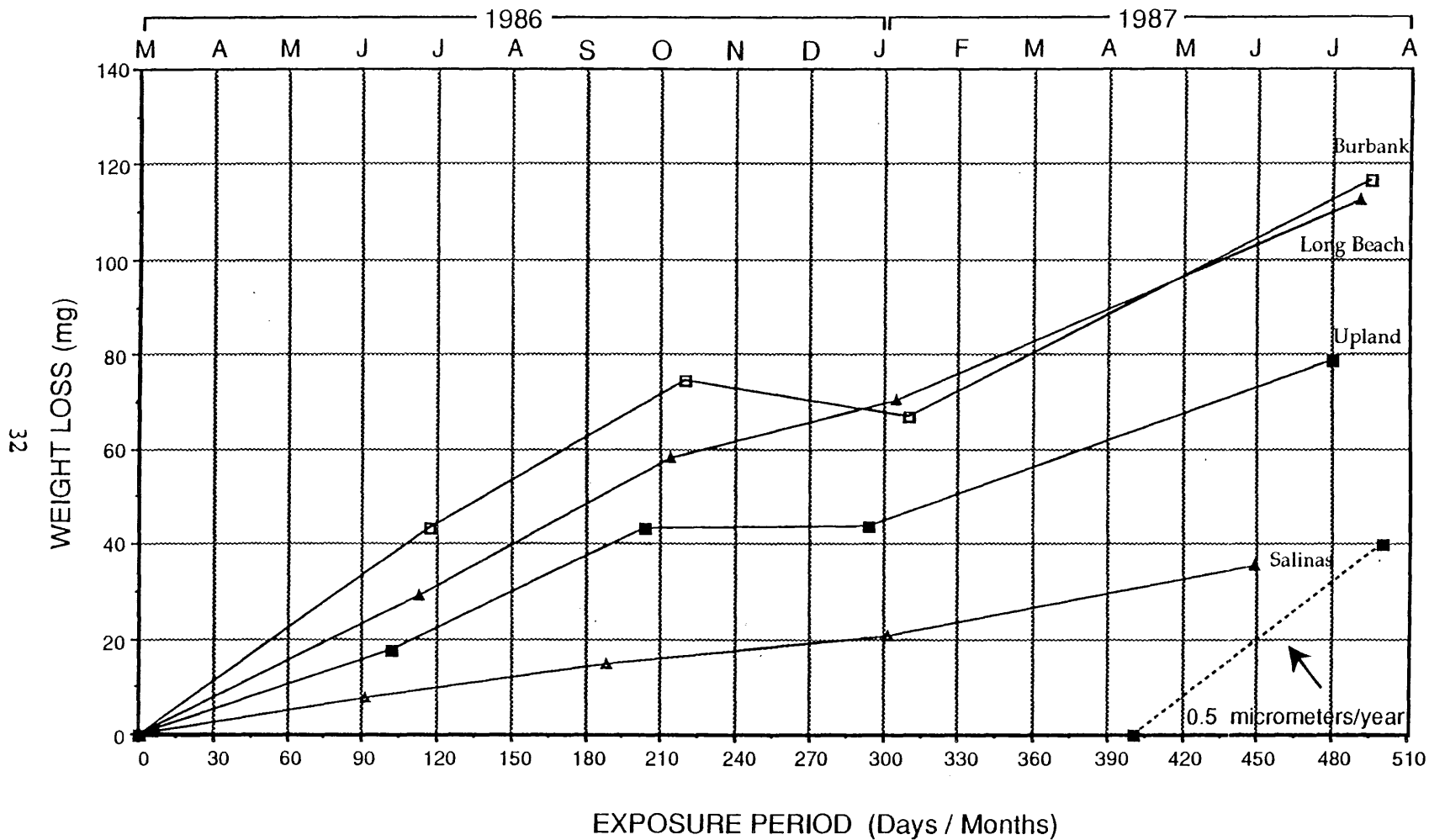


FIGURE 3-3. WEIGHT LOSS VS. TIME FOR NICKEL, FIRST SET

NICKEL / BURBANK

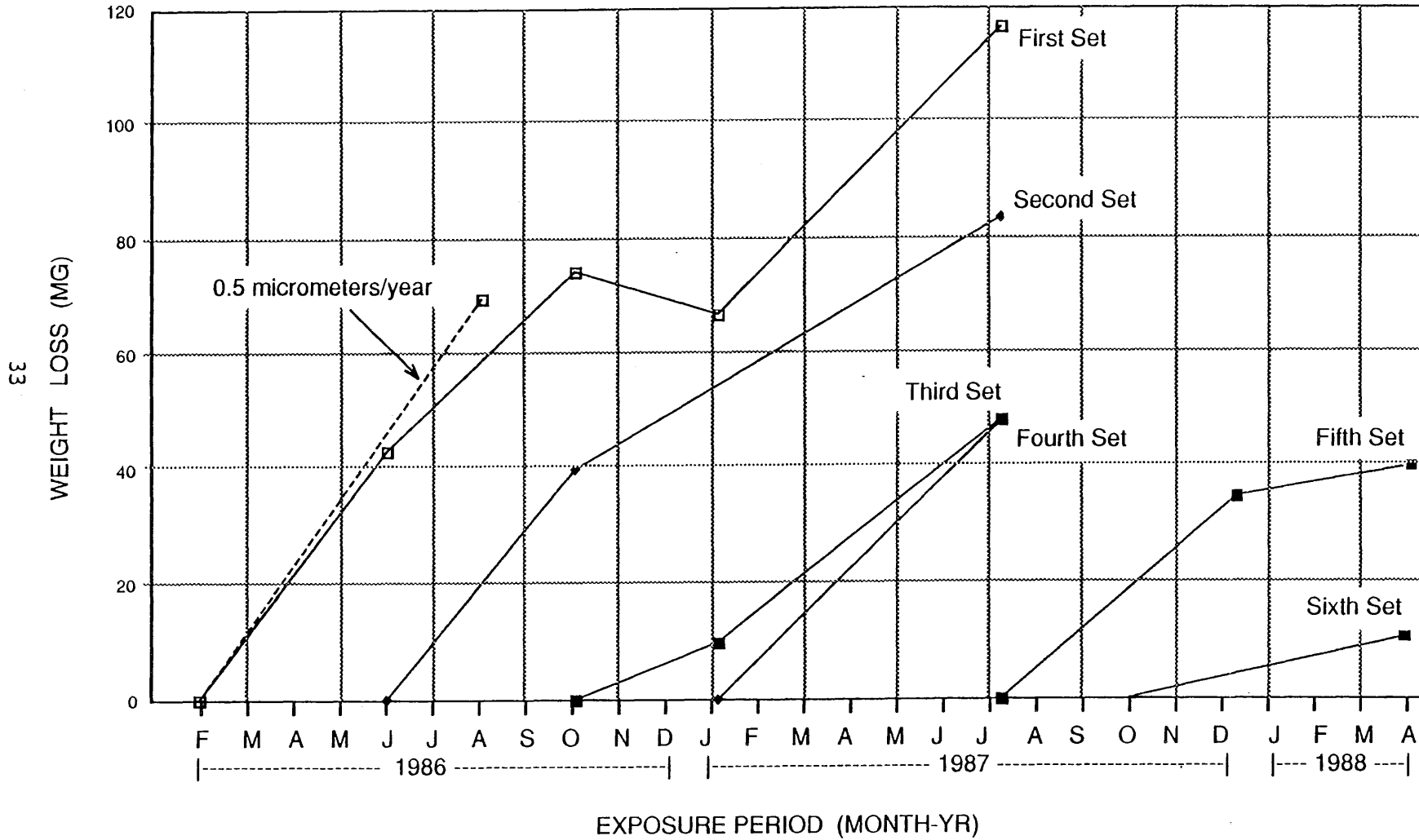


FIGURE 3-4. WEIGHT LOSS VS. TIME FOR NICKEL, BURBANK SITE

HIGH CARBONATE PAINT - FIRST SET

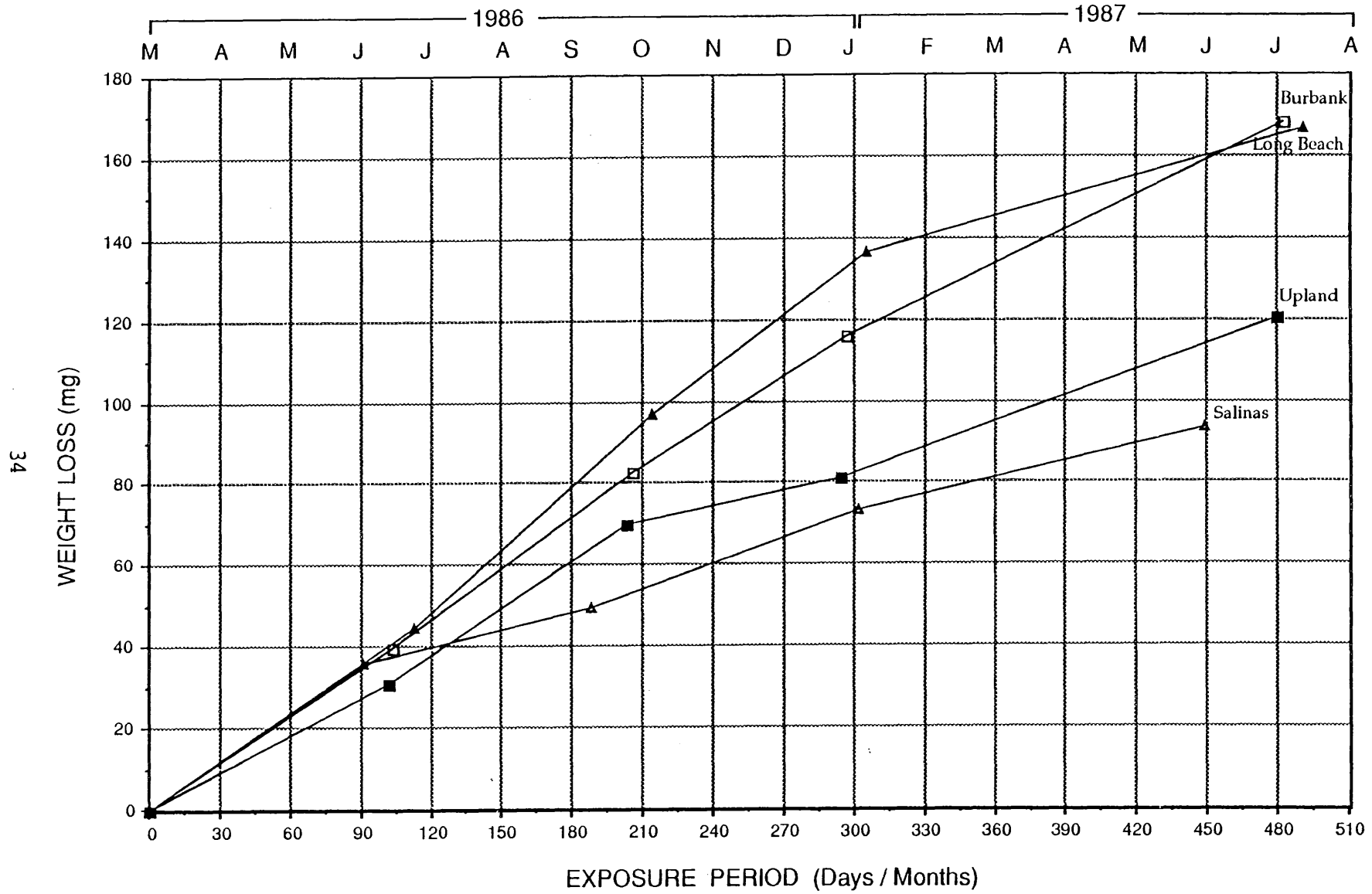


FIGURE 3-5. WEIGHT LOSS VS. TIME FOR PAINT WITH CARBONATE EXTENDER, FIRST SET.

extender much lower weight loss data were observed with very similar damage at all four sites (Figure 3-6). A closer inspection of the data in Figure 3-6 suggests that the weight loss increased with the square root of time.

3.1.1.4 Aluminum

Figure 3-7 shows the weight loss for the sets of aluminum samples at all sites with exposure beginning in July 1987. Again, there appeared to be no great difference in the corrosion loss at the four sites except for the data obtained for one year exposure. It is interesting that, although the exposure commenced at the end of the summer, the pronounced decrease in damage in the winter was still obvious and similar to the results for the other materials.

3.1.2 Strength Loss of Fabric

Figure 3-8 shows the loss of strength for the nylon samples at all sites exposed in July 1987. The damage at the background site in Salinas was much lower than at the other three sites. The damage at the three polluted sites were similar. The lower damage in winter observed for other materials was also seen for nylon.

3.1.3 Conclusions

In summary, there was a markedly lower damage rate in winter for all materials at all sites. This cannot be attributed to a possible anomaly during one year, since the data from two seasons showed the same winter effect. The reason for this behavior was not obvious and will require more extensive analyses of local pollution and weather data (see Section 4.0 - Damage Functions). As expected, the background site, Salinas, generally showed lower damage, confirming that pollution levels play a significant role in materials damage. The corrosion damage observed in this study was very small compared to that reported in other parts of the world. For example, on the basis of the corrosion rate for

LOW CARBONATE PAINT - FIRST SET

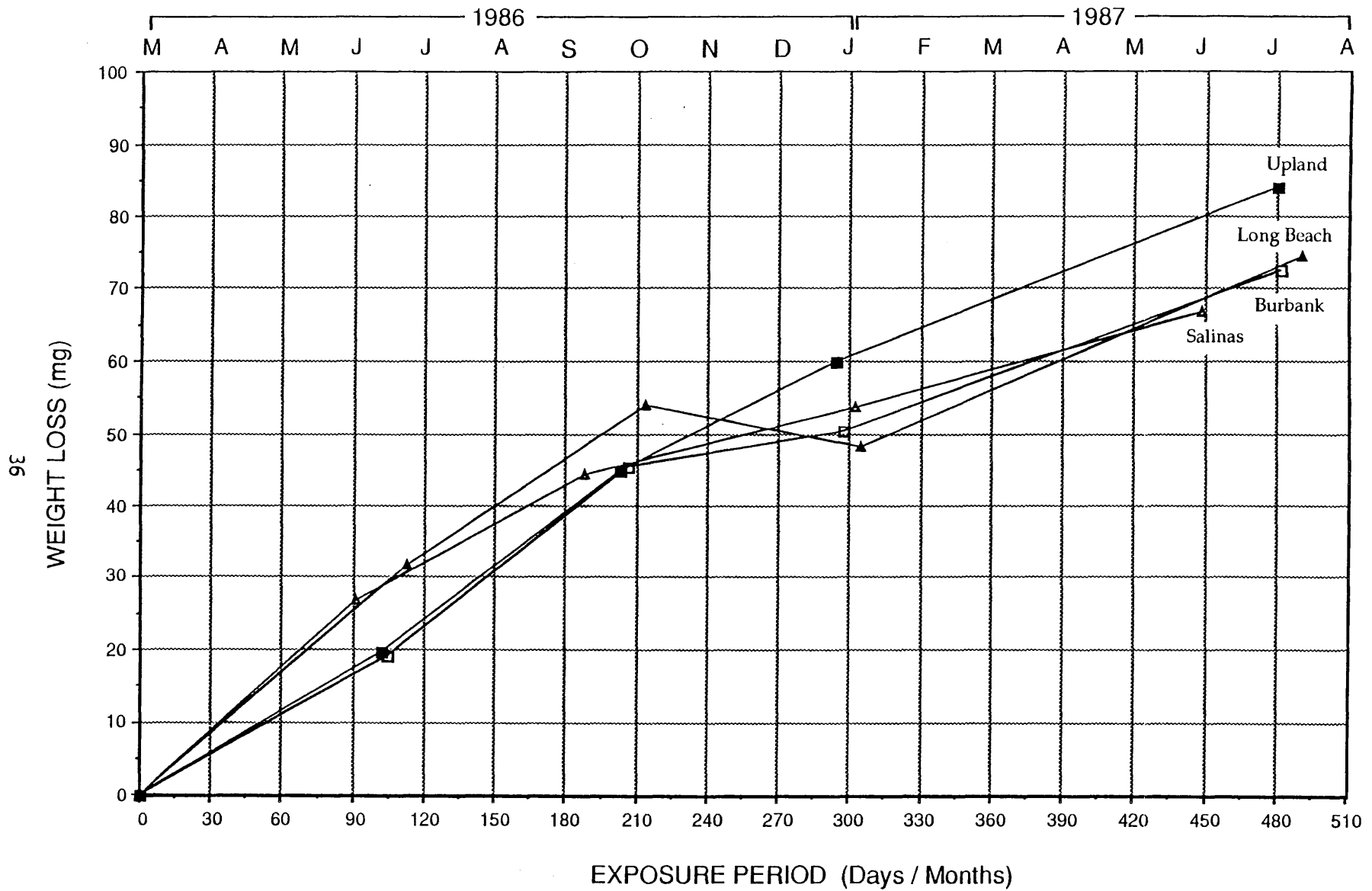
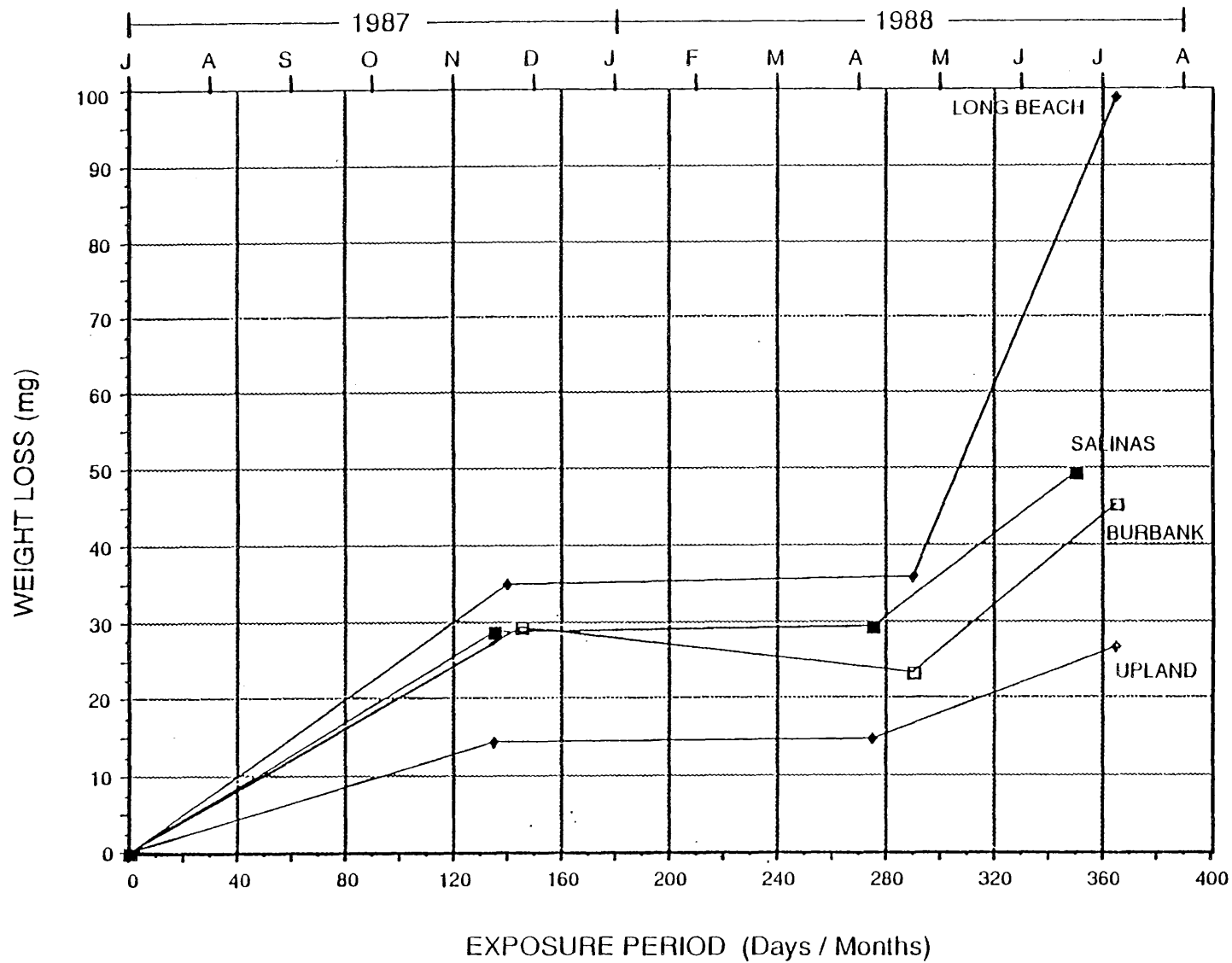


FIGURE 3-6. WEIGHT LOSS VS. TIME FOR PAINT WITHOUT CARBONATE EXTENDER, FIRST SET

ALUMINUM - FIRST SET



37

FIGURE 3-7. WEIGHT LOSS VS. TIME FOR ALUMINUM, FIRST SET

NYLON FABRIC - FIRST SET

38

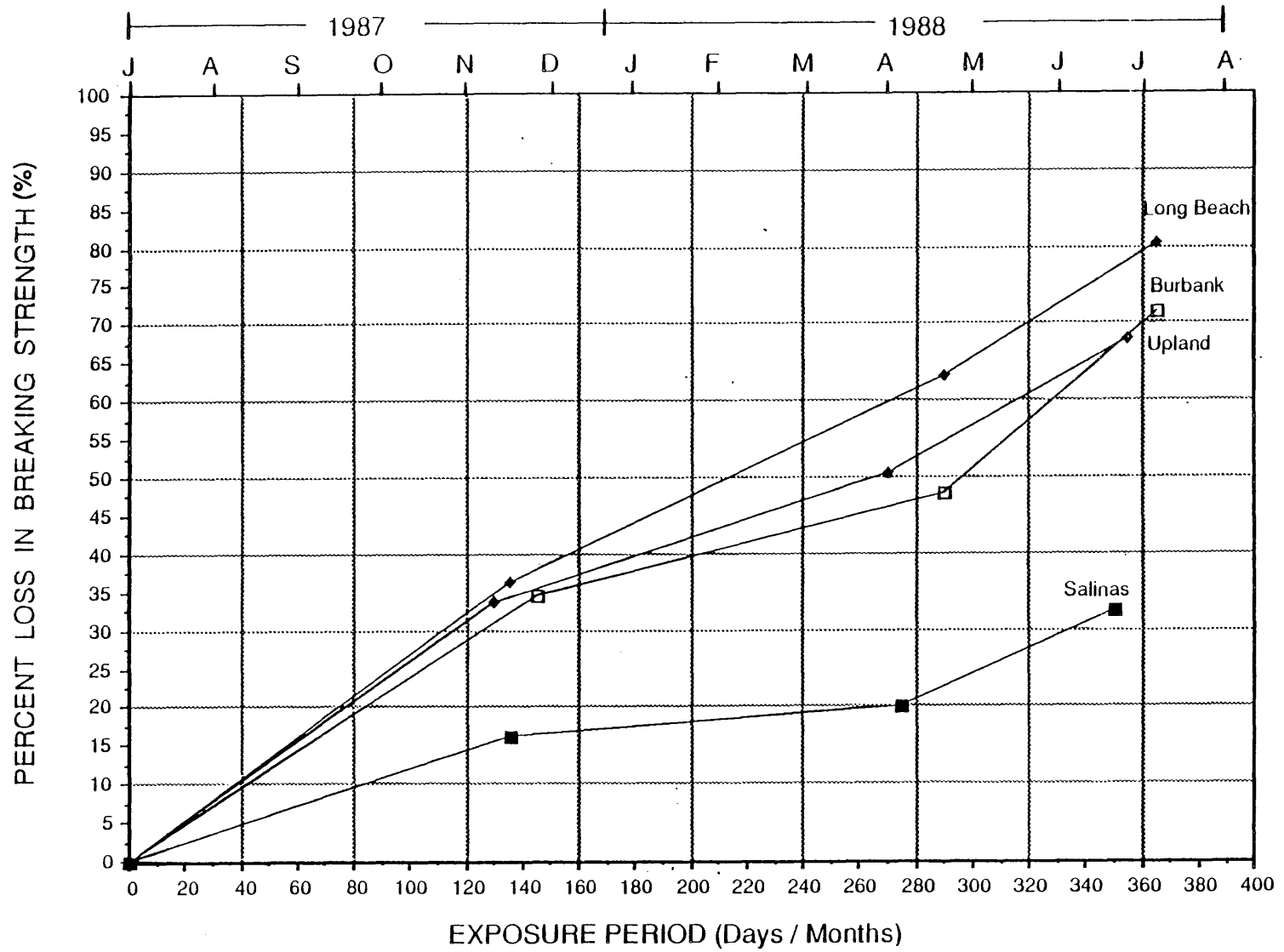


FIGURE 3-8. REDUCTION IN BREAKING STRENGTH FOR NYLON FABRIC VS. TIME, FIRST SET.

galvanized steel, the sites in our study would be classified as rural sites by ASTM and ISO. This is most likely due to the very low SO₂ levels in Southern California. SO₂ is generally believed to be the most important pollutant causing damage to materials such as zinc (18). Most damage functions for zinc and galvanized steel published so far considered only SO₂ as the pollutant causing corrosion.

3.1.4 Atmospheric Corrosion Rate Monitors (ACRM)

ACRMs were exposed at each test site between April 1986 and March 1988 providing a continuous record of the corrosion behavior. The ACRM data were collected on magnetic tape using a computerized data logger (ACRMDL). The design of the ACRMs and their mode of operation were described in detail earlier (7-9). Software for the storage, display and analysis of the ACRM data was developed at the Rockwell International Science Center (17) and was slightly modified at USC.

The instantaneous corrosion rate was obtained every 10 minutes by the measurement of the polarization resistance R_p which is inversely proportional to the corrosion rate. For the purpose of this program the ACRM data were used in a qualitative way indicating relative changes of corrosion rates rather than absolute values. In the following, R_p values are used, therefore, instead of corrosion rates.

At each site, two zinc and nickel ACRMs mounted on galvanized steel and nickel coupons, respectively, were exposed on the sample racks. One ACRM of each material faced the sky, the other faced the ground. In addition to the four ACRMs, a temperature-relative humidity (RH) probe was also exposed, and the data were collected using the data logger ACRMDL.

The ACRMDL worked quite reliably during the 24 months of the program. Occasionally some problems occurred which might have been due to extreme climatic conditions affecting the Epson computer in the ACRMDL; usually these problems could be fixed within a few days. At

Long Beach the ACRMDL could not be used for several weeks due to repairs at the test site. At Salinas one of the local operators and/or EMSI personnel did not always successfully correct problems with the ACRMDL. Therefore, there were many months at Salinas when data were available only for a few days. Table 3-1 gives a summary of the time periods for which valid ACRM data are available.

The ACRM data gave information concerning the instantaneous corrosion rate which is displayed as $\log(1/R_p)$ vs. time. 144 data points/day were collected for each sensor at each test site. Integration of the $1/R_p$ versus time curve for a 12 hour period gave the corrosion loss, INT, for this time period. Two INT data points/day were available for each sensor at each test site. From the $\log(1/R_p)$ versus time curves the corrosion time, t_{corr} , was calculated as the time for which R_p was less than a threshold value of 10^7 ohms corresponding to a very small corrosion rate. This corrosion time, t_{corr} , can be called the electrochemical time-of-wetness for which corrosion occurs and can be compared to the atmospheric time-of-wetness, t_w , which is usually calculated as the time for which RH exceeds 80%. In this project, the times for which RH exceeded 70% (T70) and 80% (T80) have been calculated as monthly averages. For the calculation of damage functions (see Section 4.0) the average values of T60 were found to be significant.

Figures 3-9 through 3-12 show the monthly averages for T70 and T80, and the values for t_{corr} and INT for zinc and nickel ACRMs facing the sky or the ground. For Burbank, Figure 3-9a shows the variations of the monthly averages of T70 and T80 between April 1986 and November 1987; Figures 3-9b and 3-9c show the coinciding t_{corr} for zinc and nickel; Figures 3-9d and 3-9e show the matching INT data. No significant seasonal effects were observed for T70, T80, and t_{corr} , nor did there seem to be any effect due to position of the ACRMs (up or down) (Figures 3-9b and 3-9c). However, a very strong seasonal effect occurred for the corrosion loss, INT, especially for the nickel ACRM with high corrosion rates in the summer months and low corrosion rates in the winter and

TABLE 3-1. AVAILABLE DAYS / MONTHS OF ACRM DATA

<u>Month/Year</u>	<u>DAYS</u>			
	<u>Burbank</u>	<u>Long Beach</u>	<u>Salinas</u>	<u>Upland</u>
4/86	24	15	0	16
5	31	21	11	19
6	21	18	7	26
7	23	26	19	19
8	27	31	31	31
9	19	26	23	27
10	28	31	0	6
11	30	30	9	27
12	26	27	2	31
1/87	21	21	8	25
2	13	27	27	28
3	29	24	27	31
4	30	30	0	30
5	5	13	0	30
6	14	12	7	18
7	30	30	1	7
8	31	31	28	31
9	30	19	30	24
10	26	29	31	27
11	22	26	22	11
12	0	23	27	15
1/88	0	21	21	0
2	0	2	29	2
3	5	0	8	31

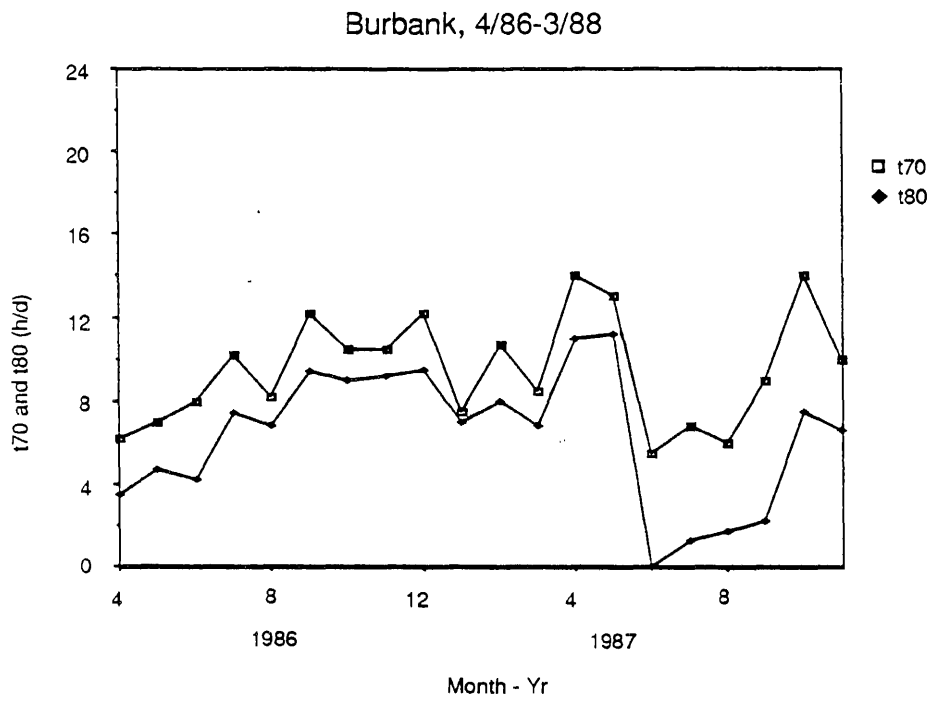


FIGURE 3-9a. BURBANK MONTHLY AVERAGES FOR t70 AND t80 FROM APRIL 1986 - NOVEMBER 1987.

Burbank, 4/86-11/87

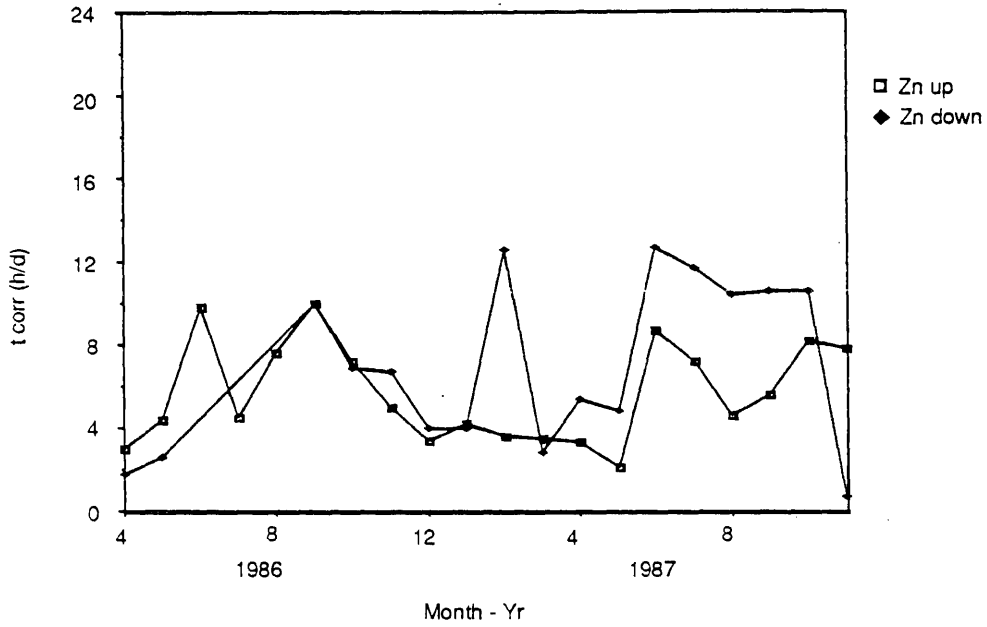


FIGURE 3-9b. BURBANK MONTHLY tcorr AVERAGES FOR ZINC, APRIL 1986 - NOVEMBER 1987.

Burbank, 4/86-11/87

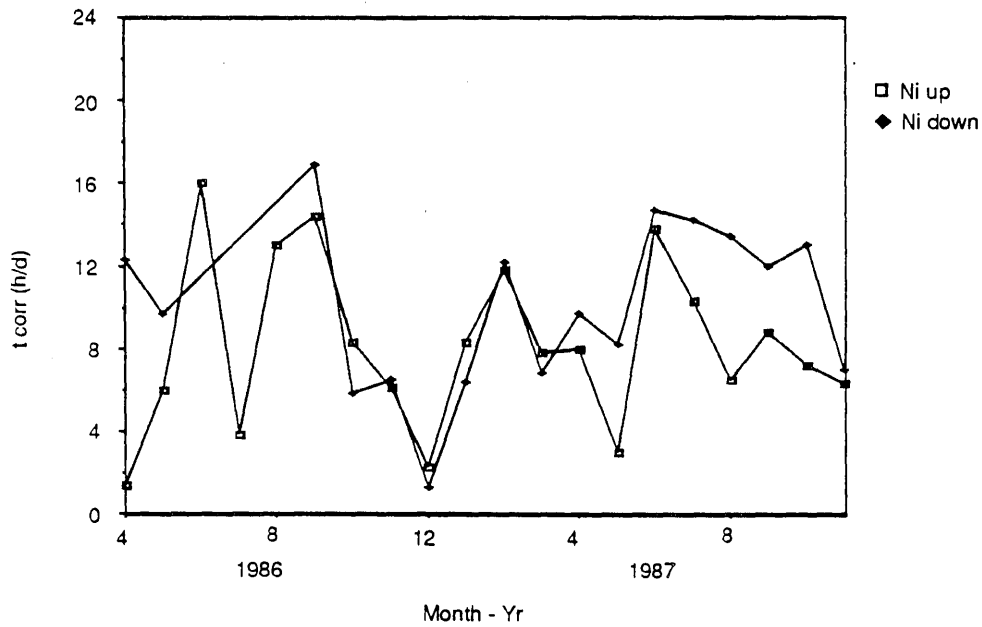


FIGURE 3-9c. BURBANK MONTHLY tcorr AVERAGES FOR NICKEL, APRIL 1986 - NOVEMBER 1987.

Burbank, 4/86-9/87

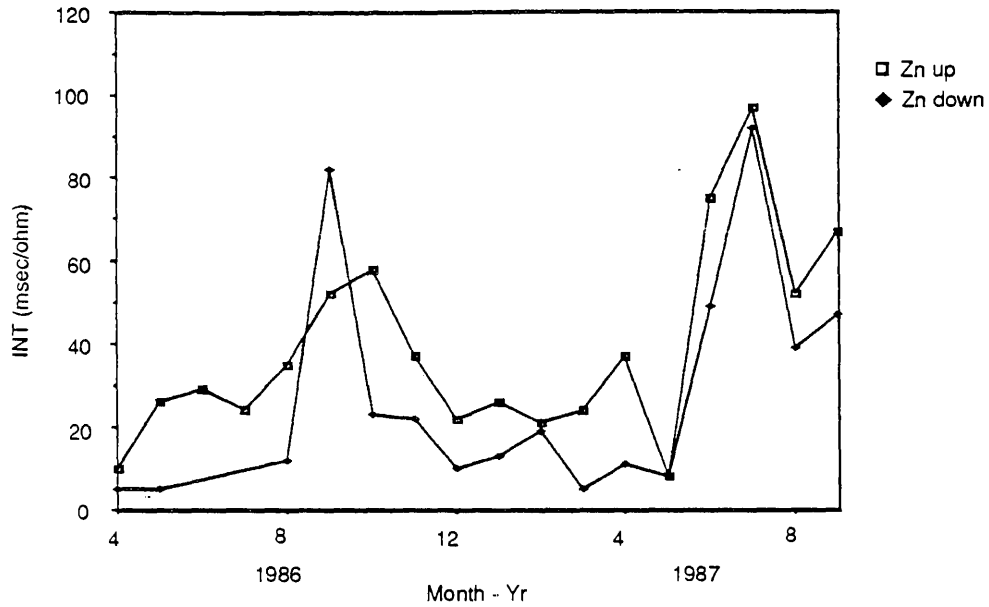


FIGURE 3-9d. BURBANK MONTHLY CORROSION LOSS FROM ZINC ACRM SENSOR FOR APRIL 1986 - MARCH 1987.

Burbank, 4/86-9/87

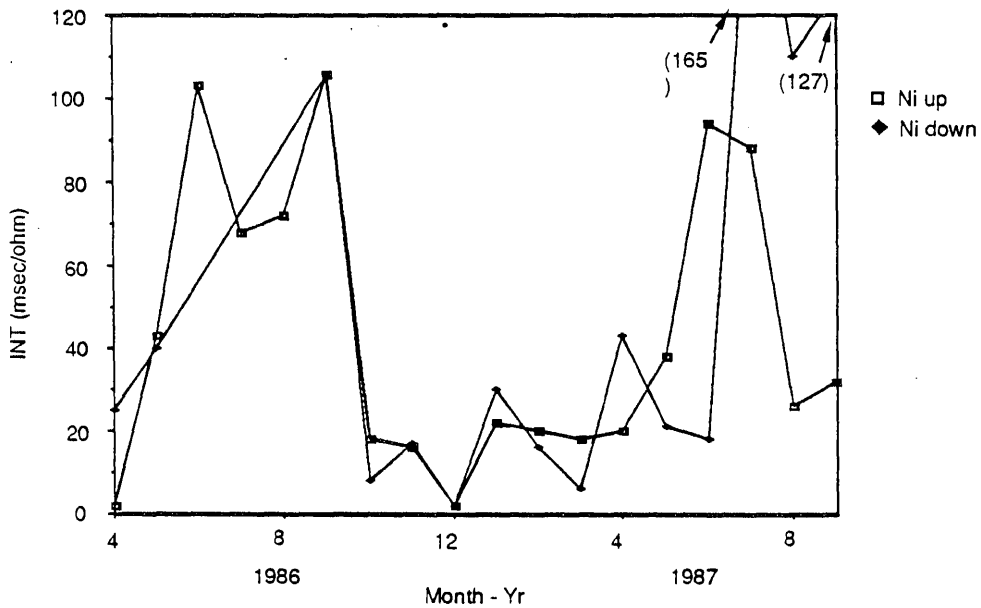


FIGURE 3-9e. BURBANK MONTHLY CORROSION LOSS FROM NICKEL ACRM SENSOR FOR APRIL 1986 - MARCH 1988.

spring of 1986/87 (Figures 3-9d and e). Corrosion rates seemed to be unaffected by the position of the ACRM (up or down). At Long Beach (Figures 3-10a, b, c, d and e), there was a slight seasonal effect for t_{corr} with the zinc ACRM facing down having somewhat higher values than the ACRM facing up (Figures 3-10b and c). As for Burbank, corrosion rates were higher in the summer especially for the nickel ACRM. It was interesting that the zinc sensor facing up had higher corrosion losses, INT, than the sensor facing down (Figures 3-10d and e) despite the fact that its t_{corr} values were lower. This result suggested that corrosion rates were higher in the shorter time-of-wetness during which corrosion was possible.

For Upland, no large seasonal effects were observed for T70 and T80 (Figures 3-11a, b, c, d and e). However, t_{corr} for the Ni sensor dropped to very low values between November 1986 and April 1987 (Figures 3-11b and c) and again around November 1987. The zinc sensor facing up had very low values of t_{corr} and INT starting in October 1986 possibly due to malfunctioning of the ACRM. The corrosion loss, INT, showed a very similar time dependence to t_{corr} with very low values in the winter and spring of 1986/87 and 1987/88 (Figures 3-11d and e).

For Salinas (Figures 3-12a, b, c, d and e) data were not available for every month of the two-year exposure program. The monthly averages for T70 and T80 reached very high values around September 1987, possibly due to problems with the RH sensor (Figure 3-12a). For t_{corr} , no particular seasonal trends were observed for the two zinc ACRMs and the nickel ACRM facing up (Figures 3-12b and c). The higher values of t_{corr} for the zinc ACRM facing up are reflected in the higher INT values for this sensor (Figures 3-12d and e). The nickel ACRM facing down malfunctioned and was not replaced.

3.1.5 Appearance Measurement

Attempts were made to differentiate the appearance damages for a limited number of paint on stainless steel samples (from the first year

Long Beach, 4/86-3/88

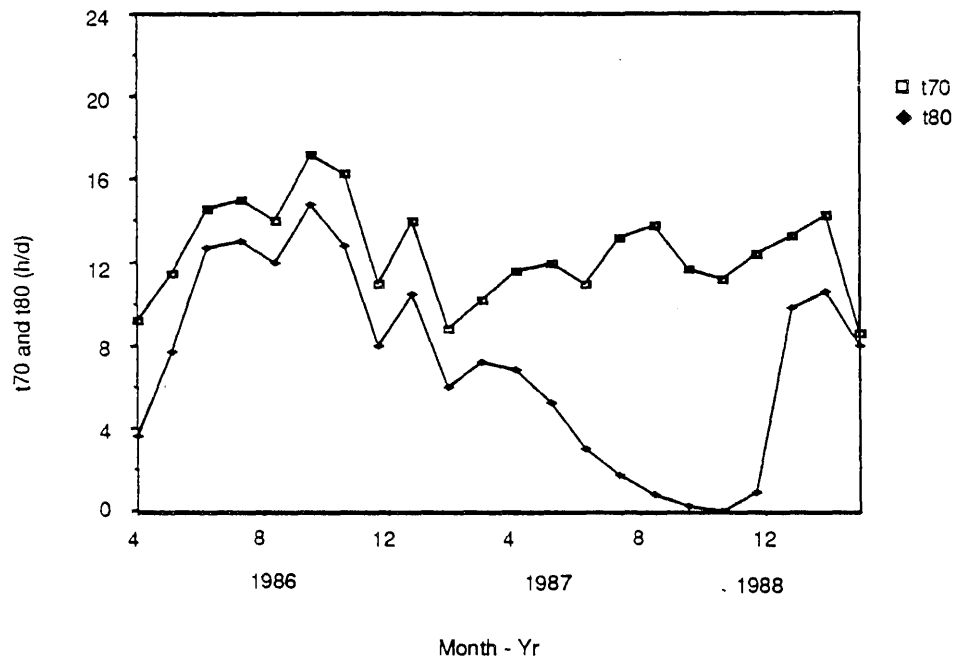


FIGURE 3-10a. LONG BEACH MONTHLY AVERAGES FOR t70 AND t80 FROM APRIL 1986 - JANUARY 1988.

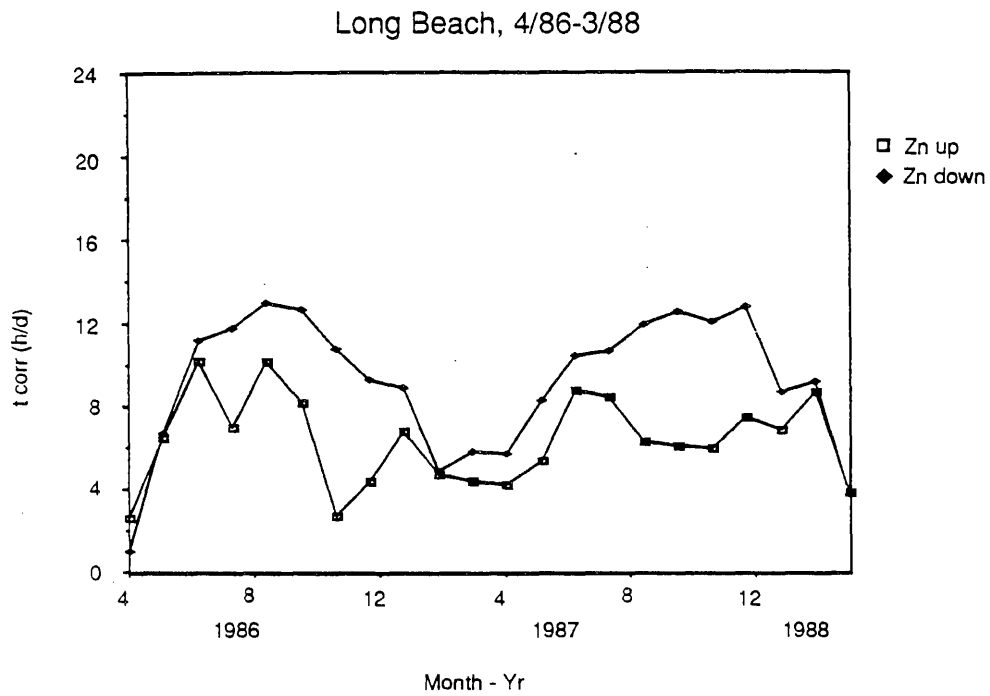


FIGURE 3-10b. LONG BEACH MONTHLY tcorr AVERAGES FOR ZINC, APRIL 1986 - JANUARY 1988.

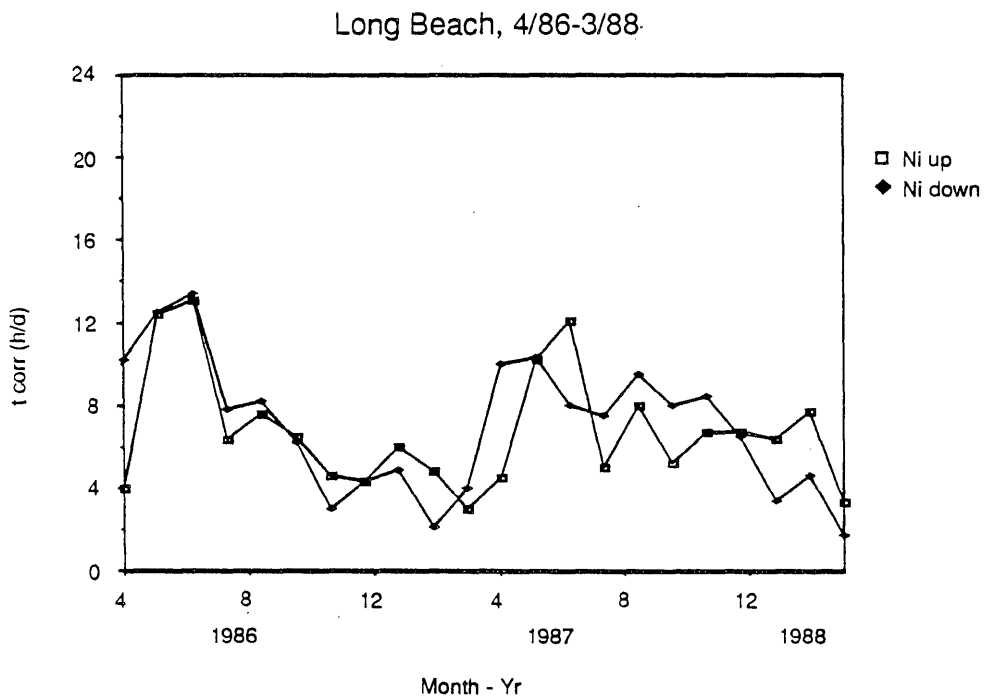


FIGURE 3-10c. LONG BEACH MONTHLY tcorr AVERAGES FOR NICKEL, APRIL 1986 - JANUARY 1988.

Long Beach, 4/86-3/88

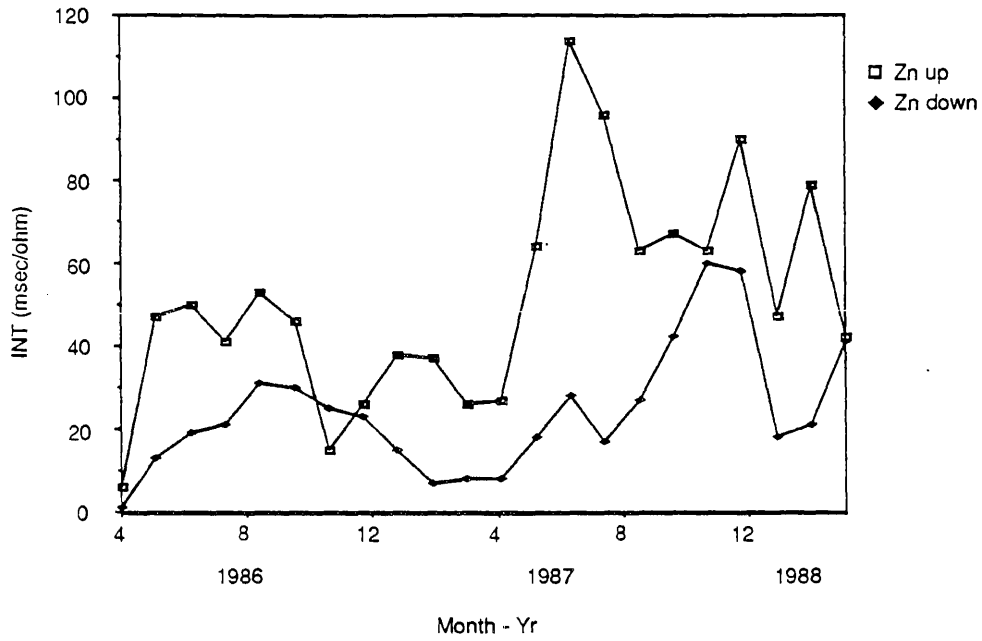


FIGURE 3-10d. LONG BEACH MONTHLY CORROSION LOSS FROM ZINC ACRM SENSOR FOR APRIL 1986 - MARCH 1988.

Long Beach, 4/86-3/88

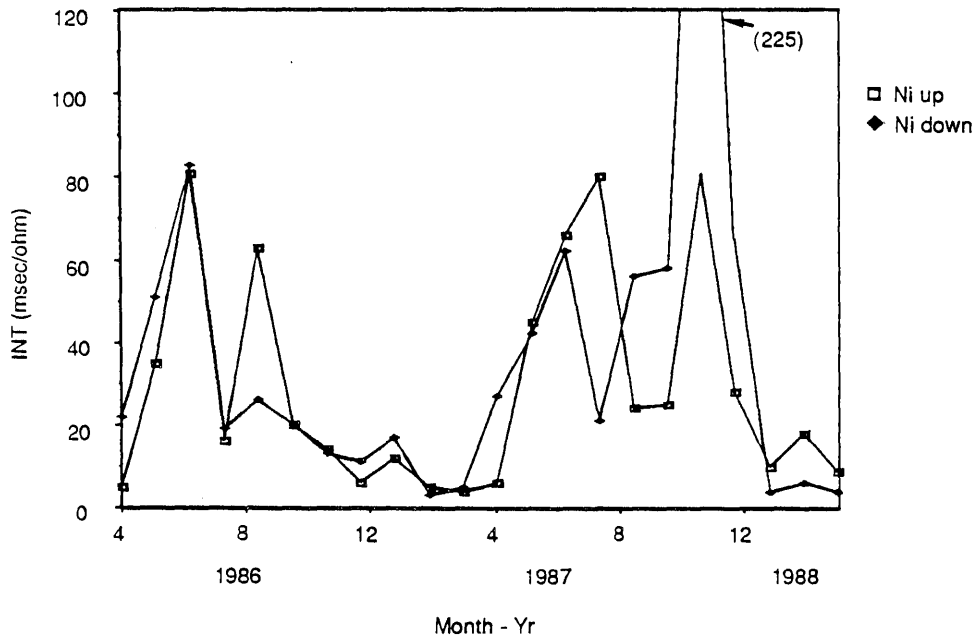


FIGURE 3-10e. LONG BEACH MONTHLY CORROSION LOSS FROM NICKEL ACRM SENSOR FOR APRIL 1986 - MARCH 1988.

Upland, 4/86-3/88

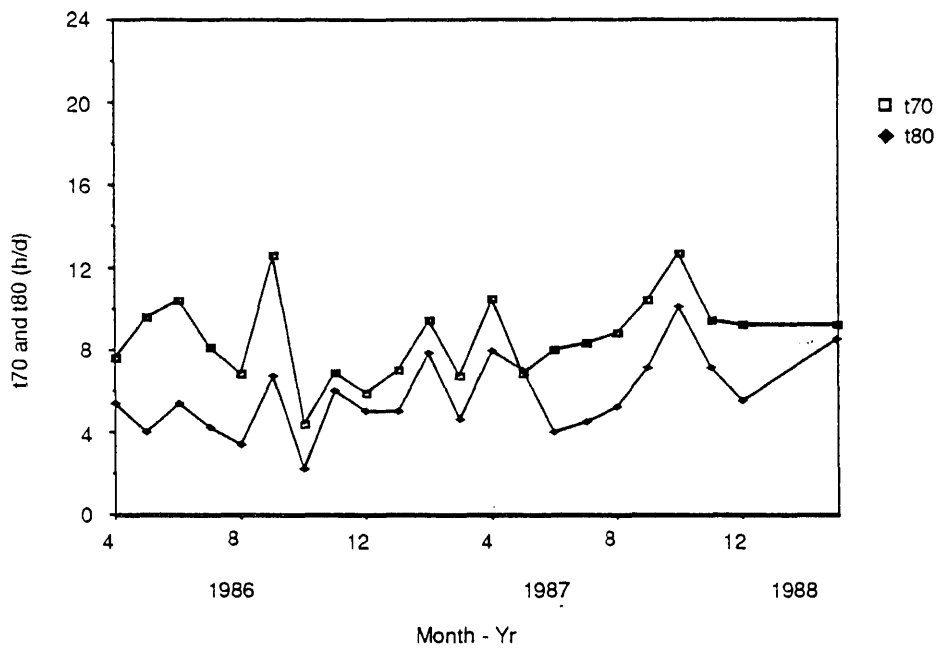


FIGURE 3-11a. UPLAND MONTHLY AVERAGES FOR t70 AND t80, FROM APRIL 1986 - MARCH 1988.

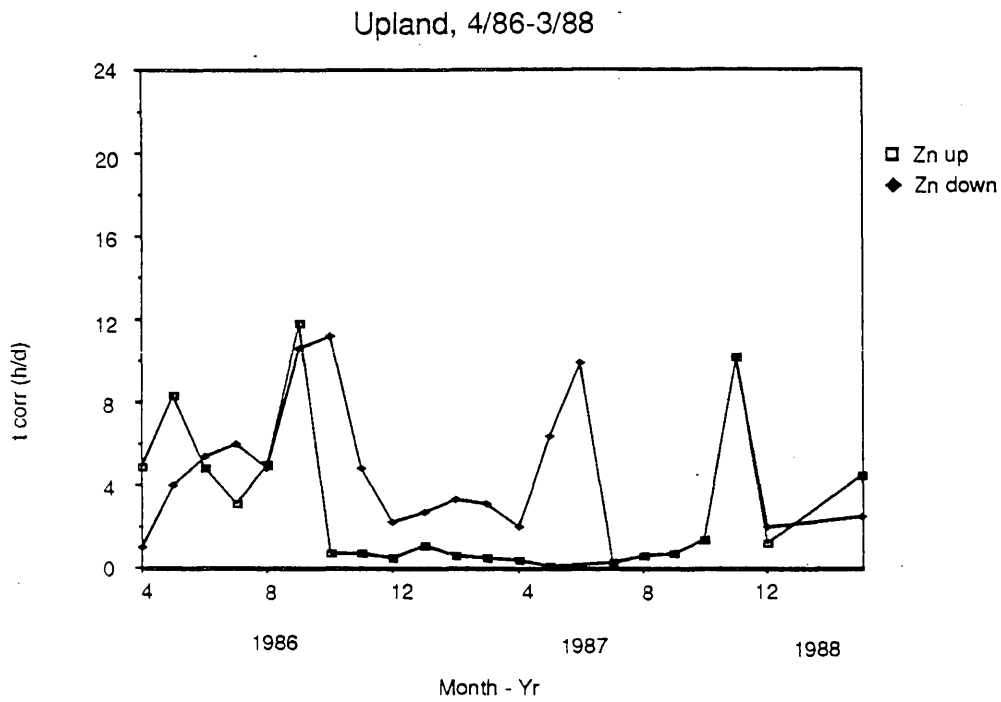


FIGURE 3-11b. UPLAND MONTHLY tcorr AVERAGES FOR ZINC, APRIL 1986 - MARCH 1988.

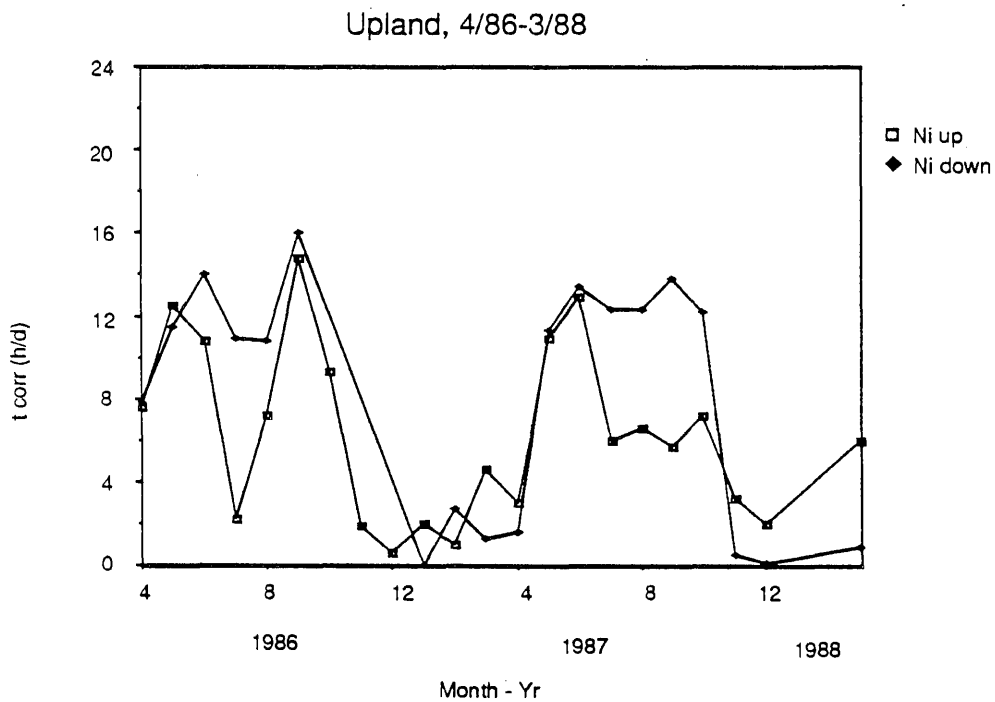


FIGURE 3-11c. UPLAND MONTHLY tcorr AVERAGES FOR NICKEL, APRIL 1986 - MARCH 1988.

Salinas, 4/86-3/88

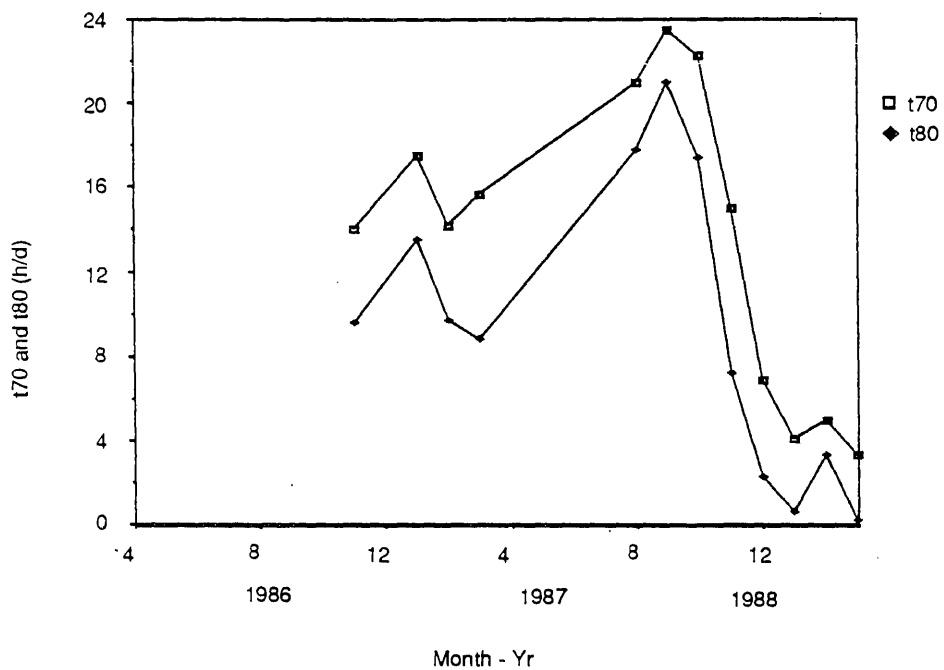


FIGURE 3-12a. SALINAS MONTHLY AVERAGES FOR t70 and t80, FROM APRIL 1986 - MARCH 1988.

Salinas, 4/86-3/88

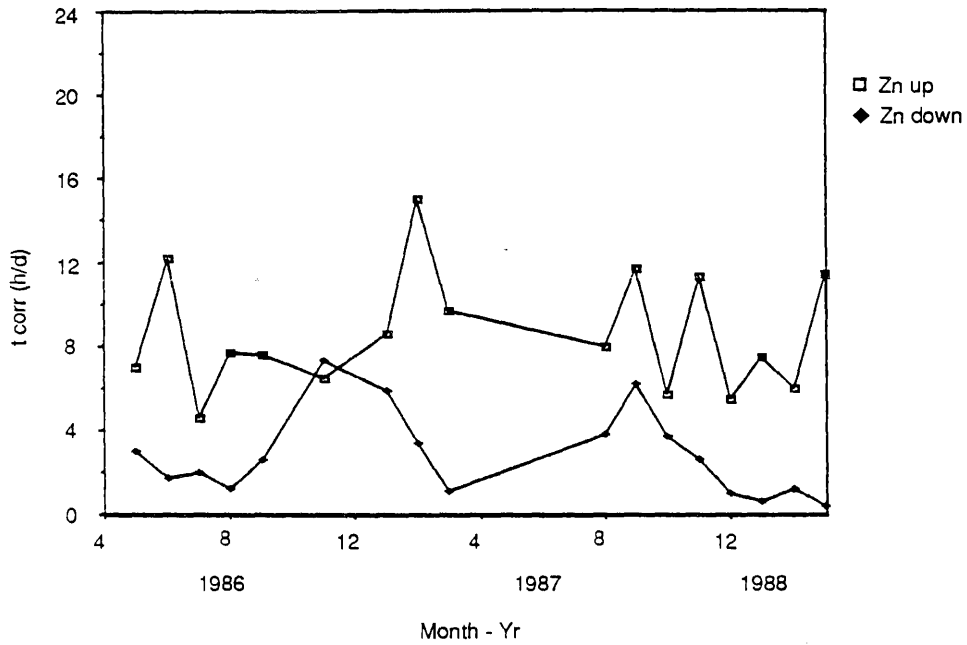


FIGURE 3-12b. SALINAS MONTHLY tcorr AVERAGES FOR ZINC, APRIL 1986 - MARCH 1988.

Salinas, 4/86-3/88

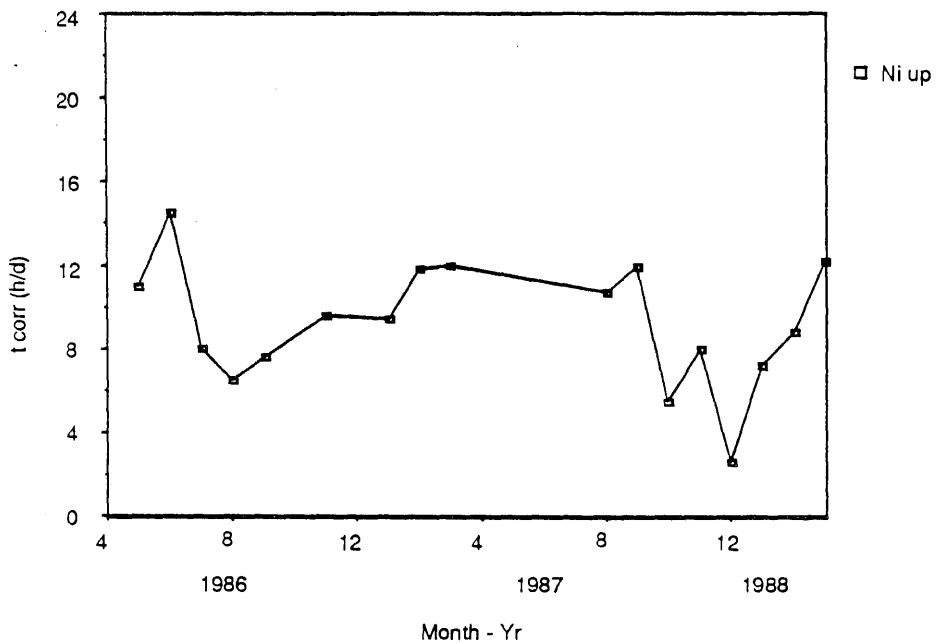


FIGURE 3-12c. SALINAS MONTHLY tcorr AVERAGES FOR NICKEL, APRIL 1986 - MARCH 1988.

Salinas, 4/86-3/88

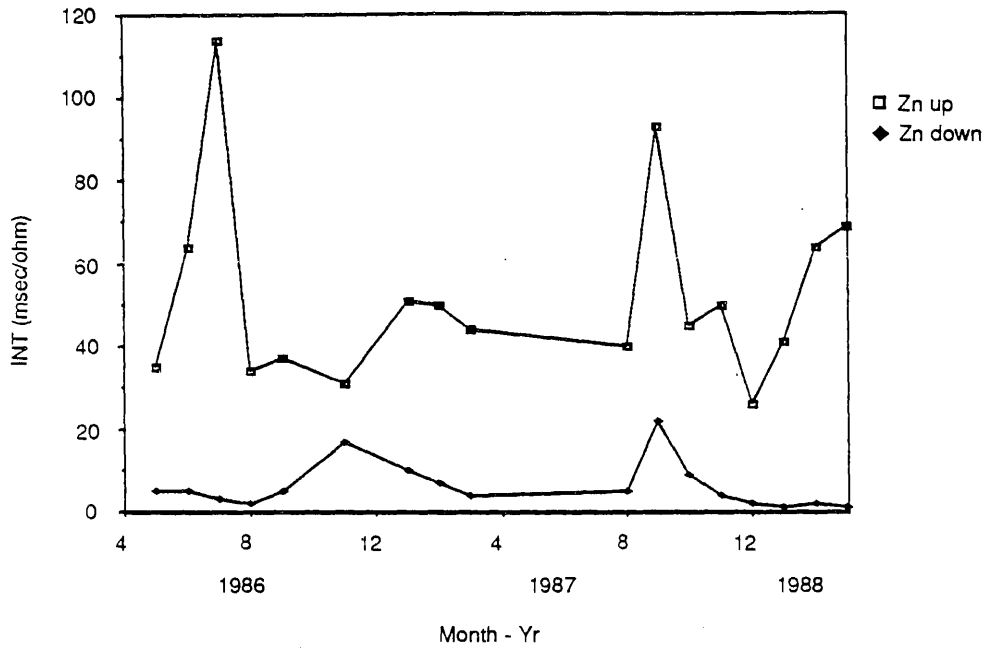


FIGURE 3-12d. SALINAS MONTHLY CORROSION LOSS FROM ZINC ACRM SENSOR FOR APRIL 1986 - MARCH 1988.

Salinas, 4/86-3/88

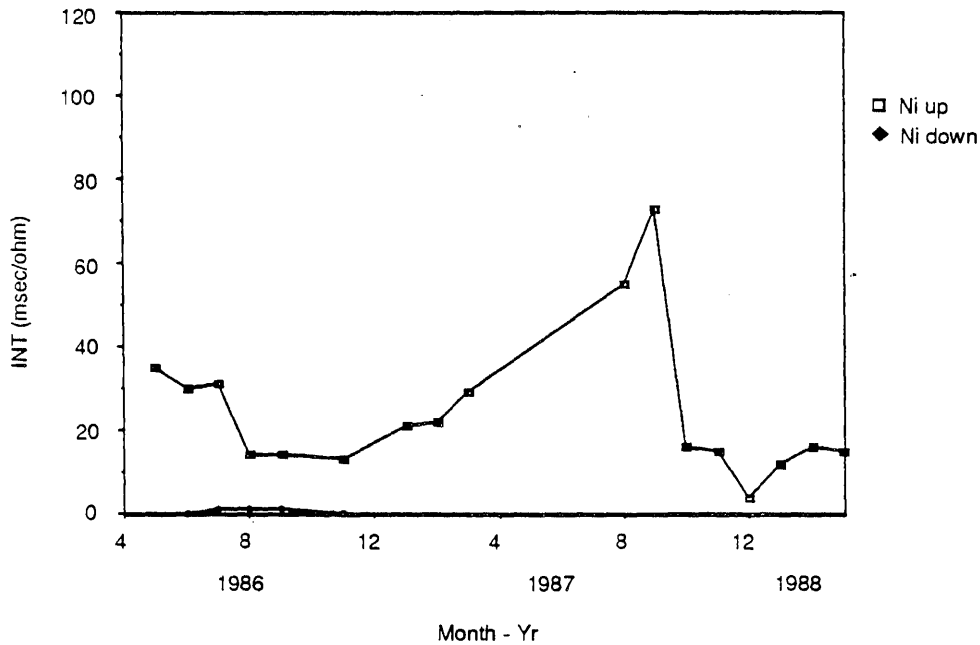


FIGURE 3-12e. SALINAS MONTHLY CORROSION LOSS FROM NICKEL ACRM SENSOR FOR APRIL 1986 - MARCH 1988.

of exposure) and all painted wood samples. The method used is described in Section 2.2 and the Appendix. The appearance measurement data were analyzed to determine the differences in damage between the two paints and between the sites, and to assess the changes with time. The experimental error and validity of the data were estimated to determine how much confidence could be placed in the results. Since the study was limited, only qualitative results were available.

3.1.5.1 Paint on Stainless Steel

Overall, the appearance damage results were inconclusive due to data inconsistencies between duplicate samples, and the correlation between exposed field samples and unexposed standards. Data inconsistencies are probably due to some expected normal variability within the samples as a result of two possible parameters: (1) sample uniformity, and (2) unstable samples changing as a function of time without exposure.

In summary, the appearance quantification method was able to detect changes in texture and color for the paint on stainless steel and indicated a somewhat larger damage to the carbonate paint. However, the method was not sensitive enough to detect differences between sites or seasons, mainly due to the large experimental variability.

3.1.5.2 Paint on Wood

The analysis of painted wood was complicated by poor sample conditions. In several cases, the wood was cracked and broken while the paint appeared intact. Due to this sample chipping, low initial gloss, and no apparent gloss change, the samples were only measured by SCI (specular component included) and hence changes in surface texture were not quantified. Similar to the results for paint on stainless steel, although the method detected damage to paint color, but was not able to differentiate between damage at different sites or seasons.